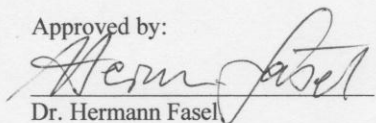


AVATAR:
AERIAL VEHICLE FOR AUTONOMOUS TARGET ACQUISITION AND
RECOGNITION

By
DIMITRI JOHN-ALLEN VERVERELLI

A Thesis Submitted to The Honors College
In Partial Fulfillment of the Bachelors degree
With Honors in
Aerospace Engineering
THE UNIVERSITY OF ARIZONA
M A Y 2 0 1 1

Approved by:



Dr. Hermann Fasel
Department of Aerospace Engineering

STATEMENT BY AUTHOR

This thesis has been submitted in partial fulfillment of requirements for a degree at The University of Arizona and is deposited in the University Library to be made available to borrowers under rules of the Library.

Signed: *Dante Sauli*



UA AERIAL ROBOTICS CLUB

SPRING | 11

FINAL DESIGN REPORT

CHRIS POOLE

MALCOLM GIBSON

JUN LI

JAMES POWELL

JOSH TOLLIVER

DIMITRI VERVERELLI



TABLE OF CONTENTS

<i>DISTRIBUTION OF WORK</i>	5
EXECUTIVE SUMMARY	6
BACKGROUND	6
OPERATIONAL REQUIREMENTS	8
CONFIGURATION SELECTION	10
POWERPLANT SELECTION	13
WEIGHT / SIZING ANALYSIS	18
WING & TAIL ANALYSIS	21
FUSELAGE DESIGN	40
TURNING PERFORMANCE ANALYSIS	44
TEST PLAN	45
BILL OF MATERIALS	AB
MANUFACTURING CONSIDERATIONS	46
COMPOSITE CONSTRUCTION	48
TIMELINE	51
CONCLUSION	52
APPENDICES	57

DISTRIBUTION OF WORK

Dist. of Work, Executive Summary, Background, Op. Requirements (Everyone)

CHRIS POOLE

Configuration Design - pg.8

Wing/Tail Analysis - pg.19

CAD Modeling - (Throughout Document)

Performance - pg.19+

MALCOLM GIBSON

Configuration analysis - pg.8

Powerplant Selection - pg.11

Performance (Turning) - pg.41

Timeline - pg.47

JUN LI

Fuselage design - pg.36

Test Plan - pg.42

Presentation

JAMES POWELL

Wing Analysis - pg.19+

Aerodynamic Performance (CFD for Wing, Tail, Fuselage) - pg.22+

Bill of Materials - pg. App B

JOSH TOLLIVER

Weight and Sizing - pg.16

Presentation

DIMITRI VERVERELLI

Manufacturing - pg.42

Composite Construction - pg.44

Conclusion - pg.48

EXECUTIVE SUMMARY

The UA Aerial Robotics Club is sponsoring an Aerospace Engineering senior design team to design and build an autonomous unmanned aerial system (UAS) for competition in the 2011 AUVSI Student UAS competition. The team will be challenged with advanced aerospace design, performance analysis, advanced composites manufacturing, and flight-testing to ensure an optimal vehicle for the competition. In order to meet all of the requirements of the competition, the aerospace team is working closely with an interdisciplinary avionics team to ensure optimal integration of vehicle systems. This document describes the background of the project, the operational requirements of the design vehicle, the high-level design of the aerial vehicle itself, the supporting analysis, and the future direction of the project.

SCOPE

The scope of this project is defined by the 2011 AUVSI SUAS Competition rules. The design vehicle must meet the following requirements: 1) The air vehicle must be able to fly continuously for 1 hour, 2) The air vehicle must fly between altitudes of 100ft and 750ft, 3) The air vehicle must be capable of carrying a three pound surveillance package, 4) The air vehicle must optimize its performance in order to meet all of the operational requirements of the competition. The design work considers advanced aerodynamics concepts, analysis of design configurations, high-level sub-system design, and highly integrated systems engineering. The air vehicle will be manufactured as efficiently as possible to meet these goals and ensure completion by design day on May 3rd, 2011.

BACKGROUND

Today's military forces are faced with complex challenges and heightened threats due to the high-risk nature of modern warfare. Quality surveillance and reconnaissance devices are necessary for ensuring intelligence that ultimately saves lives and avoids unnecessary conflict. For this reason, the military is interested in unmanned aerial vehicles (UAVs) for gathering intelligence by providing aerial surveillance of potential threats or targets.

Modern UAVs range greatly in size, shape, configuration, and mission type. Historically, UAVs were simple drones used for remote piloting of surveillance aircraft but modern advancements have promoted technologies like autonomous control and intelligent machine vision capabilities. These technologies have made UAVs extremely advantageous on the battlefield and have generated new research interest in the defense, aerospace, and computer vision industries. Consequently, many companies

have become increasingly interested in developing advanced technologies for use in unmanned aerial systems (UAS).

Small scale UAVs (figure 1) are generally employed for simple surveillance missions near the battlefield. They are usually launched by hand (figure 2), or with a small launch system with little setup requirements or complex operational needs. They are used to provide immediate intelligence about a potential threat that may be located in a region of interest. Fully capable modern UAS offer the ability to navigate GPS waypoints specified by the user and provide quality aerial surveillance of the threat. Advanced systems may even be able to recognize targets and extract information about their exact location, appearance, level of threat, or other characteristics sought by the user. This information then provides the operator with a level of intelligence and confidence sufficient to make an effective decision or strategic advance.



Figure 1: Small Scale UAVs



Figure 2: The Hand-Launched RQ-11 Raven

The Association for Unmanned Aerial Systems International (AUVSI) hosts an annual competition for university students that focuses on the development of a small scale UAS for use in a simulated military mission. The Student Unmanned Aerial Systems (SUAS) Competition requires student teams to design and construct a UAV capable of autonomous GPS waypoint navigation and intelligent target recognition. The competition

aims at simulating a real military operation involving intelligence, surveillance, and reconnaissance (ISR) objectives, air tasking orders (ATO) for departure and arrival procedures, assigned airspace for operation, and mission tasks such as target recognition and an area search. The 2011 AUVSI SUAS Competition will be the ninth annual competition and will showcase advanced UAV designs from university engineering teams across the country.

In past years, SUAS design teams have presented a wide array of UAV designs and capabilities. Top teams have engineered highly integrated systems that utilize advanced autopilot systems, effective target recognition algorithms, and high-performance aerodynamics to meet the mission objectives. However, many difficult challenges have

arisen and new solutions must be conceived to overcome them. With new improvements in design strategies, along with a growing network of new approaches, the competitors at the 2011 SUAS competition will be equipped with new aircraft and improved systems. Consequently, it is critical to consider innovative design strategies that will allow us to solve major challenges as efficiently as possible.

One of the greatest challenges for past teams was in the development of an aerodynamically optimized aircraft. Due to the integrated camera system, antennas, and other payload requirements, teams were forced to make trade-offs between avionics performance and aerodynamic efficiency. In order to compete well in this year's competition, the UA Aerial Robotics Club will sponsor an aerospace engineering team of students to design, test, and construct an efficient aircraft for use in the 2011 competition. The team will work closely with an interdisciplinary team (ENGR 498) to integrate the avionics systems into their airframe design. In order to ensure a successful vehicle, the team will focus on aerodynamics, performance analysis, composites manufacturing, and flight-testing.

In order to optimize our final product, the design process will focus intensively on background research and manufacturing techniques. By focusing on what has limited previous competitors, we will be able to identify solutions that avoid the same mistakes and allow our system to perform more efficiently and with a greater rate of success. By exploring the benefits and drawbacks of previous aircraft designs, we will recognize the benefits and limitations of each approach. Such experience will ultimately lead to more informed decisions and a highly effective design.

OPERATIONAL REQUIREMENTS

The operational requirements set forth by the 2011 AUVSI SUAS Competition Rules are presented in this section. The requirements are based on the entirety of the aircraft design and both teams must meet these objectives in their work. The aerospace team will be responsible for all aerospace and airframe related requirements and the interdisciplinary team (ENGR 498) will be responsible for aspects of electrical and computer engineering required by the competition objectives.

TEAM REQUIREMENTS AND DELIVERABLES

System Design and Development (SDD) - There are no graded events during SDD - this SOW task is entirely to aid the competitor to understand the requirements and the systems engineering process. Including in these requirements is a Plan of Action and Milestones (POA&M) to ensure completion of SDD before competition.

Fact Sheet - The team will submit a fact sheet six weeks prior to the competition. The fact sheet will provide basic descriptions of the air vehicle and systems.

Journal Paper – The team is required to electronically submit a journal paper that describes the design of their entry vehicle and the rationale behind their design choices.

Oral Presentation – The oral presentation will not be a restatement of the journal paper. Instead, it will take the shape of a Test Readiness Review (TRR) during which the competitors will present the judges with:

- Systems safety overview
- Results of development testing
- Evidence of likely mission accomplishment
- Pre-Mission Briefing
- A static display describing the elements above

Flight Demonstration – The team will demonstrate the performance of their vehicle in the form of a timed flight demonstration. During this demonstration, the vehicle will be asked to compete the tasks outlined in the subsequent section.

FUNCTIONAL REQUIREMENTS

Takeoff – Takeoff shall take place on a 100ft wide, paved runway, with no height obstacles. Takeoff from moving vehicles is prohibited. Autonomous takeoff wins the team extra points and a cash award.

Waypoint Navigation – The air vehicle shall overfly selected waypoints and remain inside assigned airspace, and avoid no-fly zones.

En-route Search – Vehicles shall search for ground targets along the predetermined flight path and identify characteristics that provide the user with “actionable intelligence”.

Landing – Landing shall take place along the same runway used for takeoff (or adjacent grass shoulder). This must be accomplished even in crosswind conditions up to a set value. Autonomous landing scores extra points and a cash award.

Total Mission Time – The total mission time (approximately 20-40 minutes) will be considered along with the accuracy of the results. Aerodynamic performance will be considered as well.

Key Performance Parameters

Parameter	Threshold	Objective
Autonomy	During way point navigation and area search.	All phases of flight, including takeoff and landing
Imagery	Identify any two target characteristics (shape, background color, orientation, alphanumeric, and alphanumeric color)	Identify all five target characteristics
Target Location	Determine target location ddd.mm.ssss within 250 ft	Determine target location within 50 ft
Mission time ⁽¹⁾	Less than 40 minutes total Imagery/location/identification provided at mission conclusion	20 minutes Imagery/location/identification provided in real time
In-flight re-tasking	Add a fly to way point	Adjust search area

Preliminary Table 1

AIRCRAFT CONFIGURATION DESIGN

The aircraft configuration is highly dependent on the operational requirements of the UAV and should optimize its performance. The configuration is mainly composed of the planform type, the tail arrangement, and the power plant.

AIRCRAFT PLANFORM DESIGN

The aircraft planform is a critical part of the design of this unmanned aerial vehicle. In order to make an informed decision, five configuration layouts were considered. In depth trade-off analysis was performed to rate the design alternatives on how well they meet the objectives of the mission. The tradeoff table and the supporting issue table are presented below.

Planform		Design Options					
Attribute	Weight	Conventional	Flying Wing	Canard	Twin boom	Asymmetric	
Stability	0.15	5	2	3	5	2	
Payload integration	0.3	3	2	2	4	4	
Ease of construction	0.15	5	4	4	4	3	
Maneuverability	0.1	5	3	3	5	4	
Transportability	0.05	3	5	3	2	2	
Payload weight/We	0.1	3	5	3	2	3	
Innovation	0.15	1	4	3	3	5	
Total Score:		1	3.5	3.15	2.85	3.8	3.5
Rank:			2	4	5	1	3

Issue Table 1: Planform Strategies	
<i>Description:</i> The planform of our air vehicle should optimize the performance objectives of the UAV. Five configurations are considered, each with varying benefits and drawbacks.	
Influencing Factors:	
IF 1: Aerodynamic Efficiency IF 2: Stability and Control IF 3: Integration with the avionics payload, including an autopilot and gimbaled camera.	
Strategies:	
ST 1: Conventional	Description: Conventional with fuselage, wings, and empennage. Benefits: Simplicity, stability, availability of design analysis, variability. Drawbacks: Ordinary, extra fuselage space, difficult to manufacture.
ST 1: Flying Wing	Description: Flying with configuration with no aft empennage. Benefits: Innovative, fuselage contributes as a lifting body. Drawbacks: Poor stability, complex dynamics, maneuverability
ST 1: Canard	Description: Configuration with control surfaces in front of the wing. Benefits: Easy to construct, good maneuverability, slightly innovative. Drawbacks: Poor stability, complex control surface analysis.
ST 1: Twin Boom	Description: Wing with twin booms extending to aft empennage. Benefits: Integrates with payload, easy to manufacture, innovative. Drawbacks: Payload weight, balancing, limits tail configuration
ST 1: Asymmetric	Description: Conventional configuration with asymmetric pod and tail. Benefits: Improved stability, innovative, payload integration. Drawbacks: Unconventional, difficult analysis, control complexity.

Preliminary Table 2

The tradeoff study showed that a twin-boom planform configuration would best meet the functional requirements of our UAV. It allows us to reduce overall weight by cutting out additional fuselage space. It also allows us to integrate the avionics payload

into the nose of our aircraft by offering the options of mounting our propulsion systems on the wings. In addition to these strong benefits, the twin boom configuration would simplify some of the manufacturing process and allow the UAV to be easily broken down into sub-components for transportation.

EMPENNAGE DESIGN

The empennage of our aircraft must provide the stability and control needed for efficient aerodynamic performance. By selecting a twin-boom planform, our decisions for the tail configuration are limited. In order to adapt well to the twin boom planform, we selected an inverted V-tail configuration. An inverted V-tail configuration replaces the conventional horizontal and vertical stabilizers with two surfaces arranged in an upside-down V-shaped manner when viewed from the tail of the aircraft. The control surfaces sometimes referred to as ruddervators, combine the tasks of both an elevator and rudder. By varying the deflection of each control surface, the tail arrangement can achieve nearly the same performance as a conventional tail. This configuration was selected mainly because of its advantageous integration with the twin boom planform. The table below summarizes the benefits and drawbacks of this tail selection.

Inverted V-Tail Configuration - Trade Off Analysis	
Advantages	Disadvantages
Integration with twin-boom planform	Complex Control System
Lighter weight than conventional tail	Induces higher stress on aft section
Smaller wetted area = less drag on tail	

Preliminary Table 3

INCORPORATING THE AVIONICS PAYLOAD

This is one of the most critical design factors for the UAV. The entire purpose of the aircraft is to carry the mission payload aloft, so several factors have been identified as essential for this purpose.

Payload Removability – Because a separate interdisciplinary design team is creating the avionics payload while the complete vehicle is still under construction, a removable payload section will be manufactured first. With size, weight and balance requirements for this payload bay, the avionics can be designed somewhat independently and in

parallel. This removable bay will also be useful for quick assembly and disassembly during missions for payload swapping or adjustments.

Aircraft Stability – Carrying a gimbaled camera as the primary data acquisition payload element means that the aircraft itself must serve as a stable camera platform. Limiting instability due to turbulence and maneuvering is very important, as is minimizing power plant vibration. Thus, the aircraft will be designed with stability as a prime concern.

Payload Field of View (FOV) – Competition requirements designate the required FOV for the camera. Since a gimbaled camera will be incorporated, some form of viewing dome will be needed. Other considerations include protecting this expensive equipment on landing, and providing adequate antenna locations for data telemetry. The aircraft will be designed with adequate FOV, camera protection, and antenna hard points.

SIZING CONSIDERATIONS

The aircraft must be sized appropriately for the mission requirements. Sizing choices are much different for small UAVs than for large, manned aircraft. They will be determined based on the following factors:

Adaptive Deployment Capability (ADC) – To appeal to the military mission nature, and with few specific sizing requirements given, the aircraft will be designed with consideration towards making it easy to launch in a variety of environments. Smaller dimensions and the potential ability to operate without large runways are key factors in achieving this. Catering towards the autopilot’s abilities will also help size to this criterion.

Transportability – The ability to take off and land in a plethora of environments is useless if the aircraft cannot be transported. In consideration of this point, the aircraft has been designed with collapsibility and/or modularity for easier transport.

Payload Capacity – Size of payload, including cameras, computers, autopilots, batteries, and more is directly tied to vehicle size. Clearly, the aircraft must be increasingly large for larger payloads. The design process is heavily coordinated with the interdisciplinary avionics team to find the best compromise in terms of weight of equipment carried vs. plane sizing.

AIRCRAFT POWERPLANT SELECTION

POWER SYSTEM SELECTION

The power systems for this aircraft also differ significantly from those of full scale. Turbine propulsion is possible, but unreasonable for this competition, so choices of propeller powerplants dominate this design.

Electric vs. Gas – Electric motors or combustion engines were considered for the aircraft. Factors such as efficiency at the selected aircraft size, weight, cost, and complexity have all been considered. The trade-off table presented below presents some of the criteria for which our powerplant must adhere to.

Propulsion Type		Design Options			
Attribute	Weight	Gas	Electric (Lithium)	Electric (Other)	
Cost	0.1	3	4	5	
Ease of Use	0.2	2	5	5	
Endurance	0.2	4	4	3	
Weight	0.2	2	5	3	
Safety	0.2	3	4	5	
Appeal	0.1	3	5	4	
Total Score:		1	2.8	4.5	4.1
Rank:			3	1	2

Preliminary Table 4

Batteries – The need for heavy batteries over lighter fuel plays a large role in the selection of gas or electric propulsion and is greatly dependent on sizing. Our current design is feasible with electric propulsion and the necessary batteries for up to a 40-minute flight time.

POWERPLANT LAYOUT

The twin boom planform configuration allows us a variety of powerplant layout options, each with their benefits and drawbacks. In order to effectively select the most optimum layout, a trade-off study was performed. The table below presents the trade-off analysis and results, and issue table for the powerplant layout.

Propulsion Layout		Design Options					
Attribute	Weight	Single Tractor	Multi Tractor	Single Pusher	Multi Pusher	Ducted Fan	
Blown wing	0.1	4	5	1	1	1	
Payload geometry	0.3	2	4	3	5	4	
Launch geometry	0.2	5	5	2	3	3	
Weight/Efficiency	0.2	5	4	5	4	4	
Power	0.2	4	5	4	5	3	
Total Score:		1	3.8	4.5	3.2	4	3.3
Rank:			3	1	5	2	4

Issue Table 1: Propulsion Layout	
Description: The layout of the electric engines, and propellers with respect to the aircraft planform configuration.	
Influencing Factors:	
IF 1: Effect on the avionics package field of view (FOV). IF 2: Available power for a large flight envelope in order to ensure high maneuverability. IF 3: Weight and size	
Strategies:	
ST 1: Single Tractor	Description: Single propeller positioned at the nose of the aircraft. Benefits: Traditional, lightweight, single engine. Drawbacks: Blinds camera from forward looking view, disturbs avionics package
ST 1: Multi-Tractor	Description: Twin propellers positioned at the forward end of each boom Benefits: Positioned away from avionics camera, high power output, integrates w/boom Drawbacks: Larger, heavier, fuselage clearance
ST 1: Single Pusher	Description: Single propeller positioned after of the fuselage. Benefits: Lighter, positioned aft of fuselage avionics. Drawbacks: ground/boom clearance, not hand-launchable, interferes w/ antennas.
ST 1: Multi-Pusher	Description: Twin propellers positioned aft of the wings Benefits: Powerful, out of way of avionics package Drawbacks: Mounting difficulties, boom interference.
ST 1: Ducted Fan	Description: Ducted fan propellers integrated into the wing structure. Benefits: Clearance, innovative, powerful Drawbacks: Difficult to integrate into body, manufacturing wing, interference w/wing

Preliminary Table 5

The trade-off decision matrix shows a multi-tractor powerplant configuration to best meet the functional requirements of our aircraft. Such a configuration allows for integration of the electric motors onto the forward booms. This allows the fuselage room to house a viewing dome for the gimbaled camera. The twin engines also allow selection of smaller propellers and increase our ground clearance.

ENGINE, SPEED CONTROLLER, AND PROPELLER SELECTION

The anticipated weight of the aircraft is approximately eighteen pounds. This weight plays a dominant role in the amount of thrust needed to meet the performance objectives of the UAV. Literature research shows that a weight-to-power ratio of about 60 watts per pound is common for an aircraft of this scale. Using this power to weight ratio, it was determined that the powerplant should provide at least 1080W to the electric motors. In order to meet this requirement, two electric brushless motors were

selected to provide the necessary power. The motor options are shown in the table below with the chosen one in red.

Motor Selection:			
Hacker Brushless Motor Info:			
Motor	Max Power	RPM/V	Suggested Propeller
Hacker A50-12S	2000	500	14x8.5 APC Electric
Hacker A30-12XL V2	500	700	13x6.5 APC Electric
AXI 4130/16	900	385	

ELECTRIC SPEED CONTROLLER



ESC	Hacker X-70 SB Pro
Manufacturer	Hacker
Applications	Airplane, Sailplane
Special Features	X-Pro Link Programming
Cont/Max Amp	70/84A
Cells NiMH/NiCD	8-16 cells
Cells Li-poly	2-6 cells
Voltage	6-20V
Programming	Fully Programmable
Type/Max BEC (A)	Switching/3A
Max #Servos/V	2-6/5V
Dimensions	75mm x 28mm x 10mm
Weight	52g

An electric speed controller is needed to control the engines' speed and direction according to the pilot or autopilot. The Hacker X-70 SB Pro is a speed controller manufactured by Hacker and designed to control Hacker's A50 series of brushless motors.

PROPELLER SELECTION

In order to meet the trust requirements of the aircraft, selection of an efficient propeller is critical to our powerplant design. In order to perform analysis on the propeller, A trial version of MotoCalc software was used to determine many of the characteristics of our propeller. Both two-blade and three-blade propellers were analyzed. A three-blade propeller was analyzed in order to increase ground clearance and fuselage clearance. The propellers and MotoCalc analysis are shown in the table below.

A 2 Blade 14 x 8.5 Propeller turning at 7000 RPM was determined to meet the requirements. The aforementioned Hacker brushless motor, Hacker electric speed controller, and the selected propeller provide the aircraft with 15 pounds of thrust under normal operating conditions.

2000ft above Sea Level, 29.92inHg, 52°F

AVATAR Works1

Motor	Hacker A50 12S	
Motor Constant (rpm/V)	500	500
No Load Current (A)	2.5	2.5
Armature Resistance (Ohms)	0.016	0.016
Battery	Thunder Power TP5000 (G4 ProLite 20C)	
Series Cell Count	5	5
Parallel Cell Count	6	6
Cell Capacity (mAh)	5000	5000
Pack Capacity (mAh)	30000	30000
Cell Voltage (V)	3.7	3.7
Pack Voltage (V)	18.5	18.5
Cell Resistance (Ohms)	0.006	0.006
Pack Resistance (Ohms)	0.005	0.005
Drive System	APC 14x8.5 2 blade	Master Airscrew 13x8 3 blade
Gear Ratio	1.00:1	1.00:1
Propeller (in x in)	14x8.5	13x8
Series Motors	1	1
Parallel Motors	2	2
Number of Propellers	2	2
Blades per Propeller	2	3
Airframe	AVATAR	AVATAR
Wing Span (in)	120	120
Wing Area (sq.in)	1569	1569
Total Weight (oz)	417.2	417.2
Static Predictions		
Current (A)	114.8	118.1
Motor Voltage (V)	17.9	17.9
Input Power (W)	2050.9	2108.9
Input Power Loading (W/lb)	78.7	80.9
Power Loss (W)	219.1	228.6
Motor/Gearbox Output (W)	1831.8	1880.3
Output Power Loading (W/lb)	70.3	72.1
Motor/Gearbox Efficiency (%)	89.3	89.2
Shaft Efficiency (%)	86.3	86.0
Motor RPM	8343	8309
Propeller RPM	8343	8309
Static Thrust (oz)	275.2	295.0
Pitch Speed (mph)	67.2	63.0
Run Time (min:sec)	15:41	15:14
Flight Predictions		
Stall Speed (mph)	29	29
Optimal Flight Speed (mph)	37	37
Throttle for Optimal (%)	67	69
Duration at Optimal (m:s)	92:32	90:42
Motor Temp at Optimal (°F)	92	93
Hands-off Speed (mph)	44	44
Throttle for Hands-off (%)	78	81
Duration Hands-off (m:s)	69:17	64:50
Motor Temp Hands-off (°F)	99	101
Best Rate of Climb (ft/min)	1137	1163
Rate of Sink (ft/min)	-286	-286

Note: Motor performance calculations take ambient temperature and heating effects into account.

WEIGHT AND SIZING

OVERALL DESIGN LOADS

For this design process, we had to choose a “starting point” for many factors, despite the fact that repeated iteration would eventually change these values. For the design of our aircraft, there were three major factors that we considered: Transportability, Adaptive Deployment Capability and Payload Capability/Capacity. Transportability is important because the UAV must somehow be moved to its takeoff point before flight operations can begin. This transportation must be simple to allow ease of use. Thus, making the aircraft able to be carried by one or two crewmembers was desirable. Not only do these decisions please customers like the military, it will also grant us points in the coming competition.

TRANSPORTABILITY AND STRUCTURES

With this said, we have gone to great lengths to make the AVATAR as transportable as possible. The aircraft was designed to split at several joints, as follows: The bend of the V tail, a split half way down the boom, and the dihedral shift at the wings. The joint at the bend of the V tail is held together with horizontal pins (Figure 3).

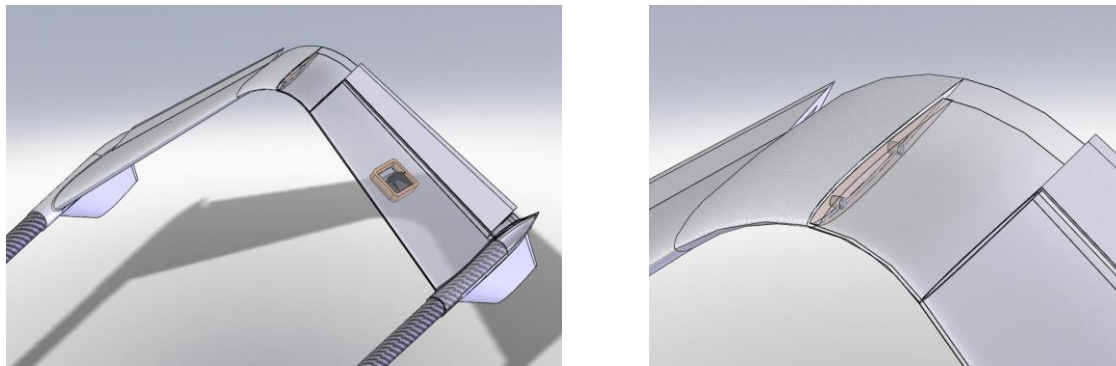


Figure 3: Tail Joiner

The wing is joined together at the dihedral shift in two separate ways: There are small pins in the rib that run along the length of the wing (similarly to the V tail pins), and two spars that run down nearly the entire length of the wing (Figure 4).

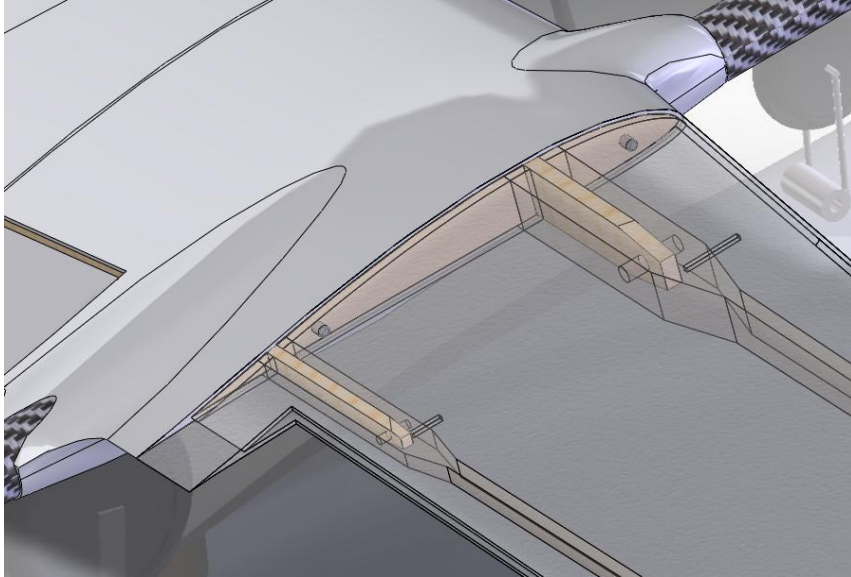
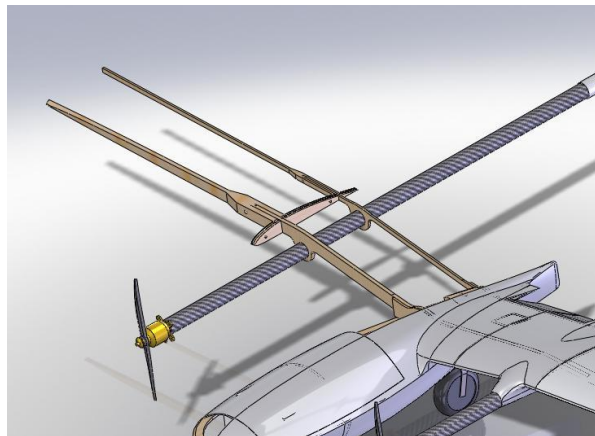
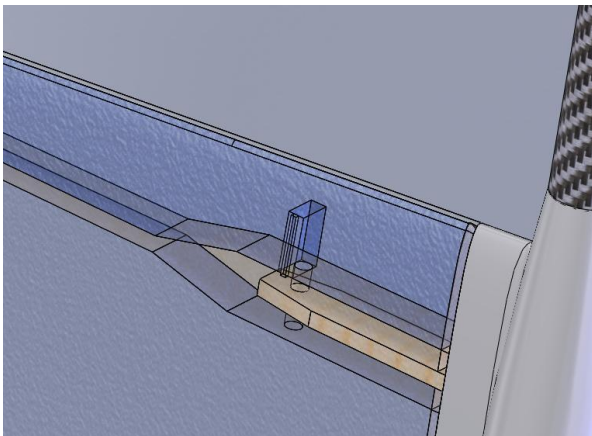


Figure 4: Spar Separation Point

These two spars split at the dihedral shift. Each outer spar, which splits into fork, acts as a female receptacle for the inner spar. Then a pin is run perpendicular to the spars length through the spar's fork, holding the spar sections at the shift together (Figure 5). This pin can be accessed through the skin of the aircraft for easy installation and removal of the wings, and prevents the outer panels from separating. The spars carry all of the bending and twisting loads (Figure 6). The booms will split at the halfway point and are connected with a carbon joiner tube and pin. This split will reduce the moment in the long booms and transfers through the joiner tube into the next boom section. With these measures in place, the aircraft should be transportable via a crate manageable by one or two crewmembers, with an assembly time of only several minutes.



Figures 5 & 6: Spar Joiner Detail

ADAPTIVE DEPLOYMENT CAPABILITY

Versatility in take-off is required by all professional UAVs. While ours will not be hand-launched, the take off distance will be short due to flaps. The flaps increase the overall wing lift at a given speed. Also, the design of the plane has been considered for strength. Given that there are several joints throughout the entire aircraft, the moments are transferred to different pins, spars, and formers. Also, when landing, the forces are transferred through the landing gear shafts to the fuselage formers. The inline landing gear supports vertical force and will keep the payload bay safe, while the tricycle gear option will allow takeoff in more rugged environments, with improved ground handling. There are also the dual spars to enhance wing strength. Accessibility was also a priority, with two large access areas at the top of the fuselage.

PAYLOAD CAPABILITY/CAPACITY

The payload that the Avatar will carry must be handled delicately. The payload bay of the AVATAR is one of its best features. A wide fuselage grants a large bay able to hold the interdisciplinary team's payload while also accommodating the batteries necessary for the required mission flight time. If for some reason the AVATAR requires more flight time, the payload bay can be filled with even more batteries. Since the quality of picture is critical to the interdisciplinary team's data processing, it is important for the aircraft to have great stability. This is due to not only its aerodynamics described in the following sections but also its sheer size and weight. The moderate airframe weight adds to this factor due to high moments of inertia and more stable gust handling. Finally, the dome was placed at an optimum angle to give the camera the required visibility of 60 degrees in all directions (Figure 7).

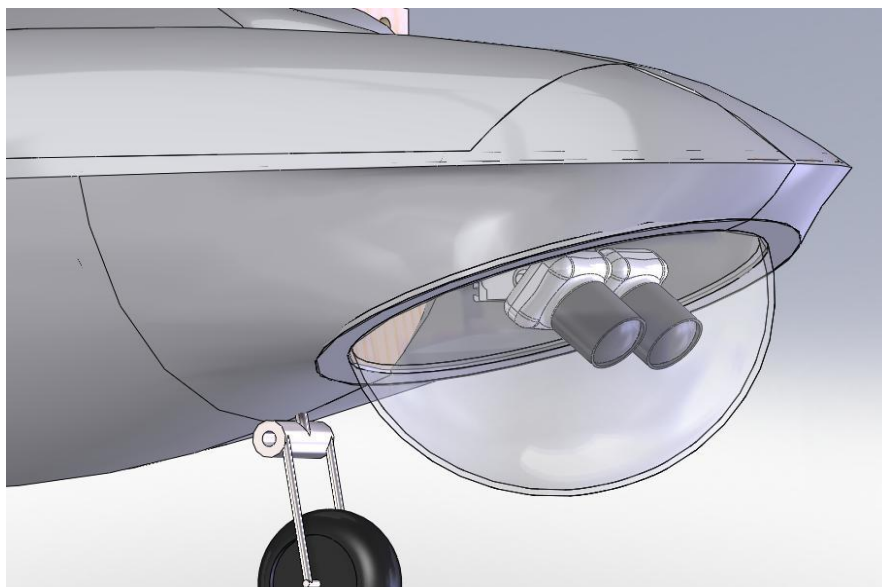


Figure 7: Payload Bay

INITIAL SIZING

To determine an initial sizing, historical/current references were used. Comparing similar UAVs and their payload capacities gives a good picture of how large our aircraft must be. Several companies produce aircraft for similar missions of roughly the same size and concept as the AVATAR. Information from a variety of these commercial vehicles, along with data from very large-scale radio controlled models, allowed the compilation of a database of sizes, weights, and payload capacities. By averaging these values, we concluded that an acceptable starting weight would be 18 pounds. The associated wing loading was approximately 36 oz. per square foot. The weight and wing loading were too heavy for one initial proposal for hand launching, but this was deemed acceptable. A tradeoff exists between short takeoff distance at low wing loading and adequate handling in windy conditions. Thus, to maintain a moderately high wing loading while still performing a short takeoff, flaps were implemented.

WING DESIGN AND ANALYSIS

AIRFOIL SELECTION

Airfoils were examined with the aid of XFLR5, a computational fluid dynamics program that uses X-Foil code written by Mark Drela. Groups of modern, low-Reynolds optimized Airfoils were compared at set Reynolds numbers which were estimated for takeoff, cruise, and sprint speeds.

	Reynolds Number	Speed
Takeoff	260,000	20 knots
Cruise	531,000	50 knots
Sprint	691,000	65 knots

XFLR5 was used to generate curves for the coefficients of lift, drag, and pitching moment as well as for C_l/C_d . The airfoils to be compared were selected by team members based on individual research into low Reynolds number flight airfoils. Comparisons were drawn based on the curves and two airfoils were selected for further optimization: the Eppler E216 and the Selig Donovan SD7034.

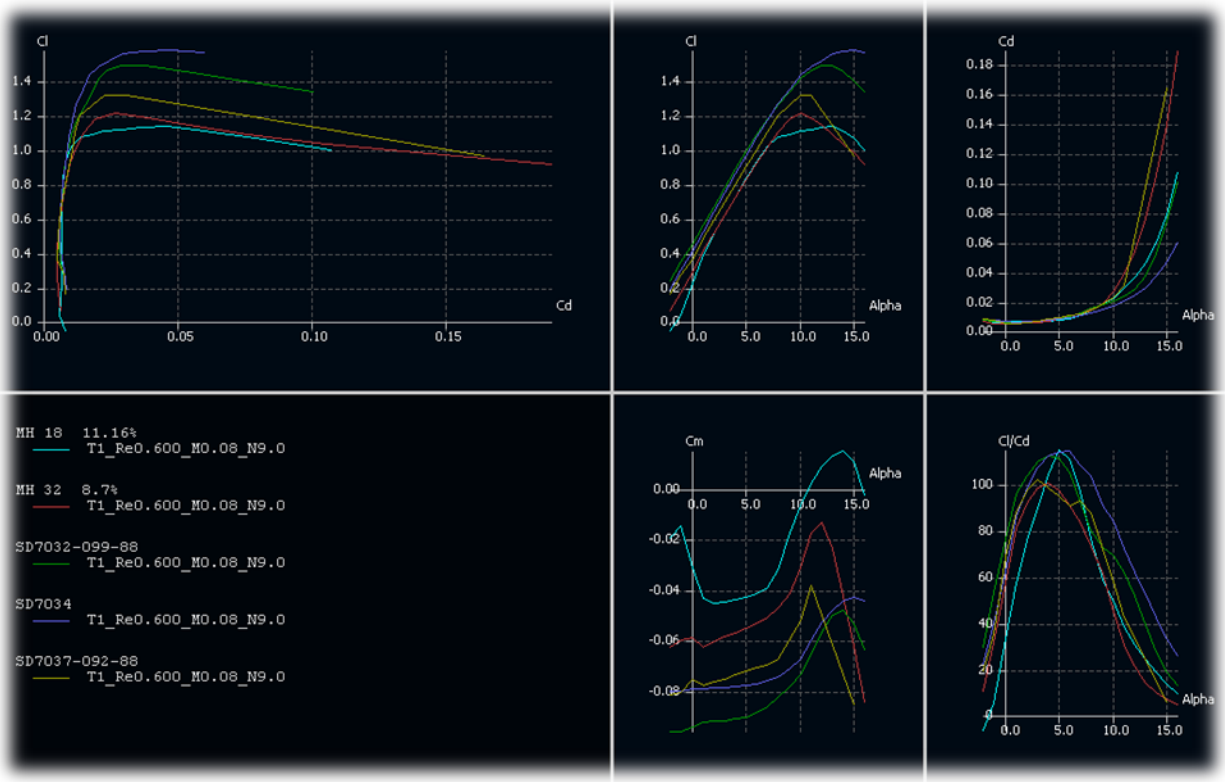


Figure 8: Comparison of 5 airfoils at Reynolds Number of 600,000 and speed of 50 knots

Data was collected from both airfoils and placed into the AVATAR Toolbox spreadsheet (ATS), which allowed for full wing comparison and optimization of both airfoils. In the end, the SD7034 was selected due to its ability to cruise at the desired velocity while generating the desired lift with a smaller incidence angle and greater L/D than the E216.

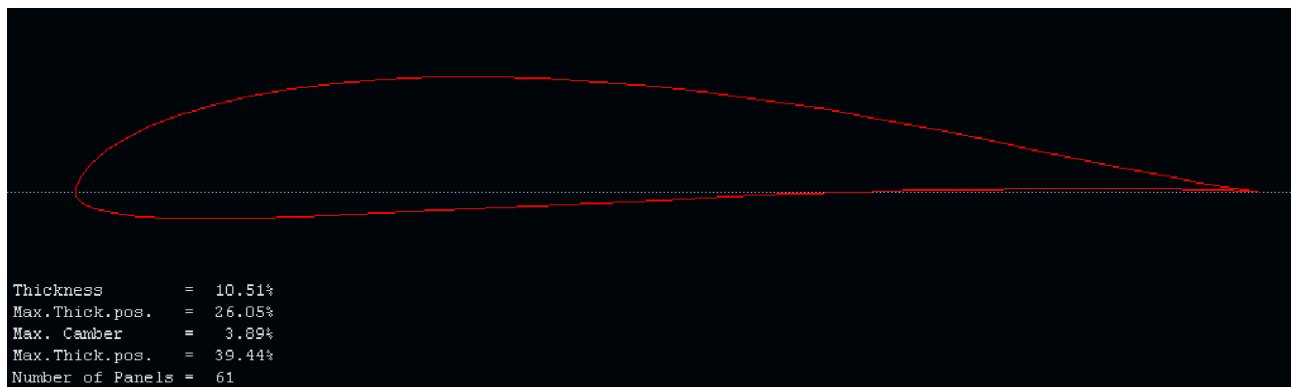


Figure 9: Render of the SD7034

For the tail, the team wanted a modern, low-Reynolds symmetric airfoil with a low drag. Using the same method used to find the SD7034, the SD8020 was selected.

PRELIMINARY PLANFORM DESIGN

Once initial airfoil options were selected, the planform for the vehicle was designed. Based on our earlier design decisions for a, a twin boom, twin tractor, inverted v-tail aircraft, the general layout could be predicted and appropriate equations selected (these will be detailed in the following). A rigorous Microsoft Excel spreadsheet (the “AVATAR Toolbox”) was used to interconnect design of the wing, tail, and control surfaces, which allowed quick changes of any variable. This made quick iteration possible to optimize various parameters.

Fixed data was the first element added. This included flight altitude, air density, and kinematic viscosity. Very general flight regimes were also included to produce some initial Reynold’s numbers and agreed with the values used for airfoil selection. Wing sizing was the first critical aspect. For an initial estimate, historical figures from various similar UAVs were consulted and a span of 96 inches was chosen. Predicting an aspect ratio of 8 and a taper ratio of 0.5 with no sweep produced values for wing area and mean aerodynamic chord using simple geometrical equations. Applying the initial weight estimate of 18 pounds to the wing area yielded an acceptable wing loading of 36 oz/ft², so the wing dimensions and weight were combined with the flight regime estimates via the lift equation (Eq. 5.71 Anderson).

$$L = W = q_{\infty} S C_L = \frac{1}{2} \rho_{\infty} V_{\infty}^2 S C_L \quad (\text{Eq. 5.71 Anderson})$$

The resulting value for C_L was then adjusted with a simple finite wing equation (Eq. 1 Simons) to produce a value of C_l required for the airfoil.

$$C_L = C_l \left(\frac{A}{A} + 2 \right) \quad (\text{Eq. 1 Simons})$$

This was next used to better refine airfoil selection. Criteria discussed in “Airfoil Selection” were again applied and the Selig Donovan 7034 airfoil was officially chosen. This concluded basic wing calculation. See ATS Table 1.

Performance Analysis Worksheet

COLOR KEY:

User Adjustable Cells

Critical Result

From outside program

Parameter

Constants

Alt (ft)	2000
Rho (slugs/ft ³)	0.0022409 lb/in ³ 4.17E-05
Mu (slugs/ft-s)	3.70E-07

Performance Desired

Vstall (knots)	15
Re stall	360000 ?
M stall	0.02
Vcruise (knots)	50
Re cruise	1210000 ?
M cruise	0.08

Initial Weight Estimates

W _e (lbs)	9	Wing loading (oz/ft ²)	36
W _{to} (lbs)	18	(Lift required)	

Initial Wing Size Estimates

Root Chor	Taper ratio	Tip Chord (in)	Span (in)	S (in ²)	AR	Sweep (in)	MAC	MAC loc (spanwise, in)
16	0.5	8	96	1152	8	0	12.44444	21.33333333
(ft)		(ft)	(ft)	(ft ²)				21.33333333
1.333333			8	8				

Regimes

	Takeoff	Cruise	Sprint
Speed (knots)	23	50	65
Speed (mph)	26.46771	57.5385	74.80005
(ft/s)	38.819308	84.3898	109.7067
Weight (oz)	18	18	18
Mach	0.03	0.08	0.10
Re	3.13E+05	6.81E+05	8.86E+05

CL req	1.332584	From Prandtl	0.281975	From Prandtl	0.166848927	From Prandtl
Cl req	1.665729	140719565	0.352468	0.28517417	0.208561158	0.167964 (Est. from CL=C _L (A/(A+2)))

SD7034	a req	-0.5
	l/d	52
E216	a req	-3.4
	l/d	36

Airfoil Comparisons

Foil:	Cl max	a max	Cd max	Cl best L/D	a best L/D	Cd best	L/D
SD7034 (50 knots)	1.6	15	0.05	1	5.5	0.008	120
SD7034 (20 knots)	1.5	14	0.045	1	5	0.012	92
SD7034 Flap (20 knots)	1.82	6	0.065	1.5	0.5	0.04	
E216 (50 knots)	1.6	12	0.04	1.05	2	0.007	147
E216 (20 knots)	1.55	9	0.022	1.1	5	0.009	120
E216 Flap (20 knots)	x	x	x	x	x	x	

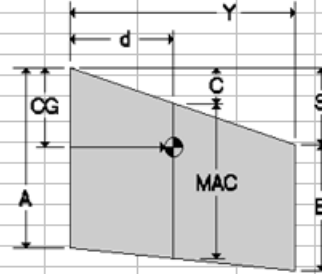


Table 1

Now a much more detailed examination of wing shape was performed. Geometric relations were applied to a system of variables which allowed for two wing panels per side. Input options included total span, section span, root chord, taper ratio, section sweep and tip vertical offset. The effect of twist was included later, as will be discussed. Again using basic geometry, for each section the following were calculated: Aspect ratio, mean aerodynamic chord (MAC) and aerodynamic center (AC) location, dihedral angle, lateral area, center of lateral area, the lift produced and the vertical lift produced. A factor called "inboard load fraction" was manually adjusted to redistribute lift between the sections by varying their incidence angles, as a method of ensuring both that flaps would be effective, and that the load distribution would be appropriately shaped. Flap sizing will be discussed shortly.

With these values determined for each section, overall wing data was assembled by Excel to give total area, wing loading, aspect ratio, taper ratio, dihedral, sweep, and the overall MAC and AC. These values provided a good reference, as did the "Visualizer" section of the spreadsheet, which graphically depicted the wing (and other aircraft geometry) describe by the inputs. See ATS Table 2.

Advanced Wing Design										Total Span (in)		120													
Inboard Panel Estimates										Half	Section	Section	Section	Section	Section	Section	Section	Section	Section	Section					
Root Chord (in)	Taper ratio	Tip Chord (in)	Span (in)	S (in ²)	AR	Sweep (in)	Tip Z offset	Actual length (in)	MAC	MAC loc (spanwise, in)	Sweep dist at MAC	LE Dist AC	Dihedral angle	Vertical Lift (lb)	Total Lift (lb)										
16	0.9	14.4	17	258.4	1.118421	-0.75	3	17.2626765	15.2140351	8.350877193	-0.368421	-4.17193	10.0079798	7.2	7.311251										
(R)	Tau	(R)	(R ²)	1.118421																					
1.333333333	0.13	1.416667	1.794444																						
																* Correct when view from top/pre-corrected for dihedral									
Outboard Panel Estimates										Half	Section	Section	Section	Section	Section	Section	Section	Section	Section	Section					
Root Chord (in)	Taper ratio	Tip Chord (in)	Span (in)	S (in ²)	AR	Sweep (in)	Tip Z offset	Actual length (in)	MAC	MAC loc (spanwise, in)	Sweep dist at MAC	LE Dist AC	Dihedral angle	Vertical Lift (lb)	Total Lift (lb)										
14.4	0.7	10.08	43	526.32	3.513072	-4.32	1	43.0116263	12.3670588	20.23529412	-2.032941	-5.12471	1.332219854	10.8	10.80292										
(R)	Tau	(R)	(R ²)	3.513072																					
1.2	0.08	3.583333	3.655																						
																(If on outer panel)									
Total S (in ²)	1569.44		Ving loading (oz/ft ²)		Total AR	Total Taper Ratio	Inboard load fraction (by area)		Total MAC (in)	Sweep dist at MAC		MAC loc (spanwise, in)		Total LE Dist AC (in)											
Total S (ft ²)	10.89689		26.4247		9.17525	0.63	0.32928943		13.304538	-1.845462		27.9039		-5.314											
Total Dihedral (degrees)	1.90915243																								
																Inboard load fraction (SPECIFY)		(Adjust to shift load to inner panels and minimize tip stall)		(From LE)					
																0.4									
																Inboard load fraction FLAPS (SPECIFY)									
																0.355									

AVATAR Visualizer

Propeller		
Diad (in)	14	3 (offset)
center	17	y
left	10	2.25
right	24	2.25

Inboard Panel		
x	LE	
0	0	
17	-0.75	

Outboard Panel		
x	TE	
17	-0.75	
6.0	-5.07	
	-15.15	

Front Inboard		
x	y	
0	0	
17	-15.15	
17	3	

Front Outboard		
x	y	
17	3	
6.0	4	

Prop Front		
x	y1	y2
10	3	3
10.7	6.05123	-0.0512
11.4	7.2	-1.2
12.1	7.999	-1.999
12.8	8.6	-2.6
13.5	9.06218	-3.0622
14.2	9.41561	-3.4156
14.9	9.67757	-3.6776
15.6	9.85957	-3.8596
16.3	9.96491	-3.9649
17	10	-4
17.7	9.96491	-3.9649
18.4	9.85957	-3.8596
19.1	9.67757	-3.6776
19.8	9.41561	-3.4156
20.5	9.06218	-3.0622
21.2	8.6	-2.6
21.9	7.999	-1.999
22.6	7.2	-1.2
23.3	6.05123	-0.0512
24	3	3

Sub-Redder		
LE		
40	3	
47	-1	
TE		
52	3	
53	-1	

Fuselage		
Top		
-20	0	
20	0	
Bottom		
-40	-1	

Tail		
x	LE	TE
0	-46	-53.2
17	-40	-52

Front		
x	y	
0	14.9035	
17	3	

MACtail		
x	y	
9.20833	-42.75	
9.20833	-52.55	

ACtail		
x	y	
27.9039	-1.8455	
27.9039	-5.314	

Side		
Inner LE		
x	y	
0	0	
0.75	3	
Inner TE		
x	y	
16	0	
15.15	3	
Outer LE		
x	y	
0.75	3	
5.07	4	
Outer TE		
x	y	
15.15	3	
15.15	4	
Tail LE		
x	y	
40	3	
46	14.9035	

Boom		
x	y	
17	2.25	
17	-52	
16	2.25	
16	-52	

Contrail		
x	y	
0	7.97944	
0.75	3	
Contrail		
x	y	
8.96647	3.47059	

ContFus		
x	y	
40	3	
46	14.9035	

ContWing		
x	y	
10	10	
10	-10	

NacOG		
x	y	
3.24464	3.24464	

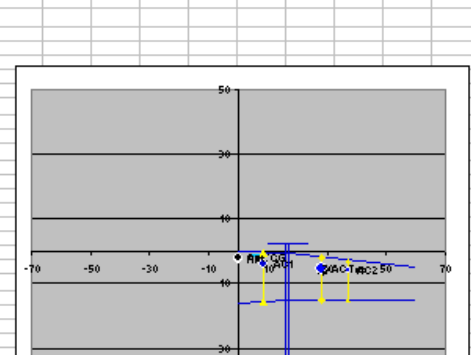
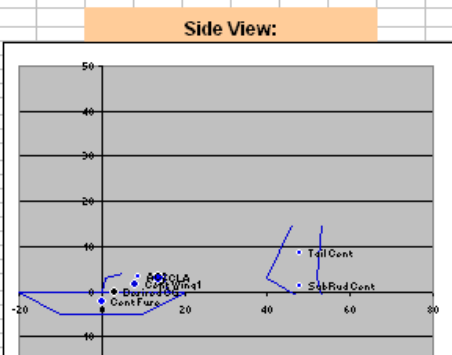
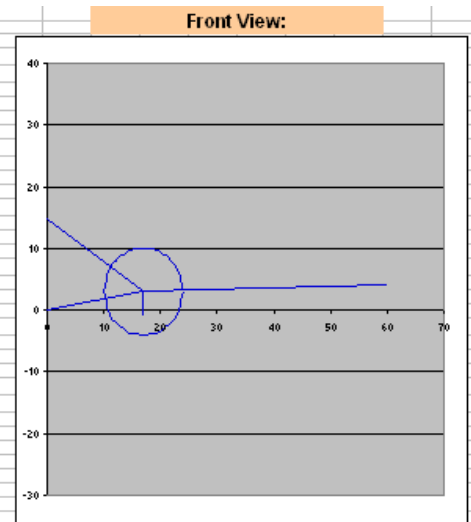
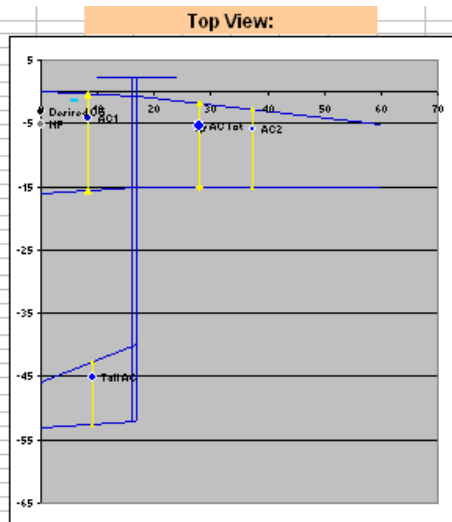


Table 2

To actually predict the performance of the wing, the section data above was again fed through the flight regime information. Wing and section lift coefficients (C_L and C_l , now using the more detailed taper compensated finite wing equation 5.70 from Anderson were again found, and using XFLR5 results for slope and zero lift angle of the SD7034 airfoil, the required angle of attack (α) for each section was displayed.

$$\alpha = \frac{\alpha_o}{1 + (\alpha_o/\pi AR)(1 + \tau)} \quad (\text{Eq. 5.70 Anderson})$$

Comparing these required α values to the stall angles and drag and moment coefficients of the airfoil in each regime gave a picture of the effectiveness of the configuration's performance. Values could then be adjusted as necessary to optimize the angle of attack of the airfoil for the critical flight regimes of takeoff with flaps, takeoff without flaps, and cruise. Changes at this stage included increasing span to increase wing area for takeoff at lower speeds (and thus shorter runway lengths), and increasing aspect ratio to improve L/D.

The next planform design factor examined was twist. Due to taper, the Reynolds number at the tip of the wing is significantly lower than at the root or MAC. For acceptable stall behavior, the root must stall before the tip, so a slight degree of twist is necessary. By displaying the Reynolds numbers at various points along the wing in each regime of the Toolbox and including the calculated stall angles of attack from XFRL5, the difference in α was used as a baseline for twist amount. Twist was applied linearly and displayed as "actual outer α ," which was compared to desired optimal α . Values were adjusted until a twist of 1.5 degrees in the outer panel was finalized. See ATS Table 3.

Regimes	Takeoff (flaps)	Maneuvering		Cruise		Sprint			
Speed (knots)	18.68	32		50		65			
Speed (mph)	21.4963836	36.82464		57.5385		74.80005			
(ft/s)	31.5280293	54.00947		84.3898		109.70674			
Weight (oz)	18	18		18		18			
Mach	0.03	0.05		0.08		0.10			
Re Tot MAC	2.12E+05	3.63E+05		5.67E+05		7.37E+05			
Re inner MAC	2.42E+05	4.15E+05		6.48E+05		8.42E+05			
Re outer MAC	1.97E+05	3.37E+05		5.27E+05		6.85E+05			
Re tip	1.60E+05	2.75E+05		4.29E+05		5.58E+05			
Per-Section Calculations:									
		Inner	Outer	Inner	Outer	Inner	Outer	Inner	Outer
	CL req	1.623357	1.426416	0.623303	0.452159	0.255305	0.18520444	0.151068	0.10958843
	Cl req	1.977212	1.737343	0.759169	0.55072	0.310956	0.22557489	0.183998	0.13347627
	Cl req	1.733687	1.506954	0.638915	0.459951	0.257886	0.18649858	0.151968	0.11004025
SD7034	Cl/a	0.075	0.075	0.107	0.107	0.107	0.107		
	Cl0	1.1	0.95	0.4	0.4	0.4	0.4		
	a req	8.45	7.43	2.23	0.56	-1.33	-2.00		
	Diff:		-1.02		-1.67	l/d	24		
(section = section MAC)	a max	10	9.5	12	13	15	14.5		
(tip a max)			9 XX		12		14.5		
	Desired tip washout (degrees)		-2		-1		-1.5		
	Linear washout at outer MAC		-0.941176		-0.470588		-0.70588235		
	Actual outer a		7.74		1.53		-2.03		
	Actual outer Cl						0.21		
	Actual outer l/d						24		

Table 3

Other remaining wing details were dihedral and sweep. Based on Lennon, 2 degrees overall was recommended for high-wing aircraft of this size. Prop clearance was a priority for the boom mounted motors, so most of this dihedral was applied to the inner panel, with the outer panel having only gentle dihedral, creating an overall effect of approximately 1.9 degrees. Sweep was used only minimally near the end of the design process, when it was found that the CG tended to be located slightly rearward. This was compensated by minimally sweeping the outer panels, which also served to push the center of lateral area aft.

At this stage of progress, wing drag estimation was completed. This was accomplished with the general drag equation Eq. 5.63 Anderson, including estimated efficiency factors. Estimations for skin friction and profile drag were employed as well, to find a general estimate of the wing drag for each flight condition.

$$C_D = c_d + \frac{C_L^2}{\pi e AR} \quad (\text{Eq. 5.63 Anderson})$$

$$D_i = q_\infty S C_{D,i} = q_\infty \frac{C_L^2}{\pi e AR} \quad (\text{Eq. 5.72 Anderson})$$

$$C_f = \frac{0.074}{Re_c^{1/5}}, \quad C_f = \frac{D_{f,top}}{q_\infty S} = \frac{D_{f,bottom}}{q_\infty S} \quad (\text{Anderson, compiled})$$

This drag computation was later compared with computational analysis of the entire airframe. See ATS Table 4.

Wing Drag Calculations							
<small>(for above regimes and alphas)</small>							
SD7034	Cd	0.05	0.042	0.008	0.008	0.007	0.007
	d						
	e	0.769231	0.833333	0.769231	0.833333	0.769231	0.83333333
	Cdi	0.118851	0.084704	0.017522	0.008511	0.00294	0.00142796
	CD Total	0.168851	0.126704	0.025522	0.016511	0.00994	0.00842796
	D wing Tot (lb)	1.79381		0.74864		0.79869	
	Actual Wing L/D	10.0345		24.0435		22.537	

Table 4

DESIGN OF CONTROL SURFACES

Flap chord location was designed to optimize control effectiveness in all regimes without stalling the surface. Deflection for takeoff was optimized to increase lift without unduly increasing drag, with the intention of shortening the takeoff run as much as possible. Landing deflections allow for major degradation of the L/D, which is desirable for making the approach angle steeper while still keeping airspeed fairly low.

To optimize the flaps for these conditions, XFLR5 was used to test different variations of the flaps. The SD7034 was run with flaps of varying chord percentages and deflection angles. From this analysis and research, the flaps were placed at 75% chord and given a deflection of 15° for takeoff and 30° for landing. These surfaces, and all others, will be actuated using Hi-Tech HS-5685MH Metal Gear, High Torque Servos. These servos are capable of providing greater than 150 ounce-inches of torque.

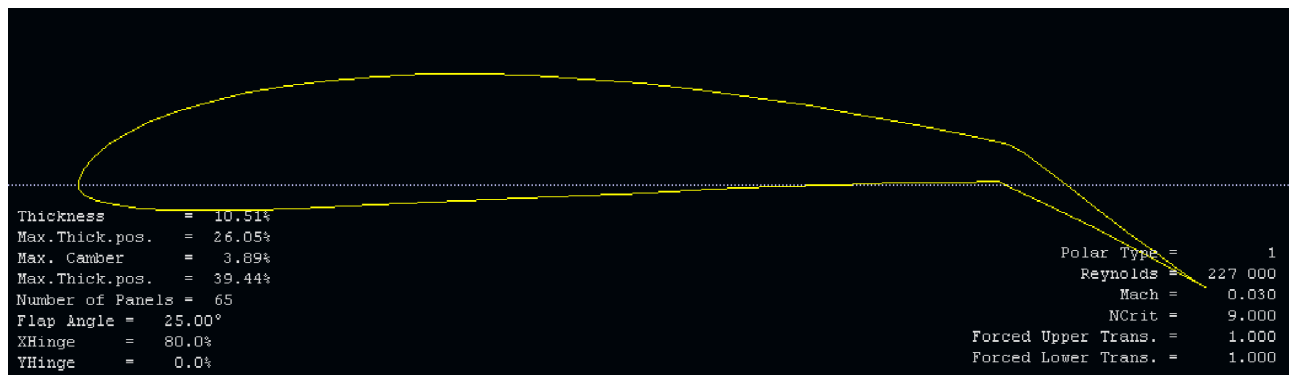


Figure 10: Example of Flapped SD7034

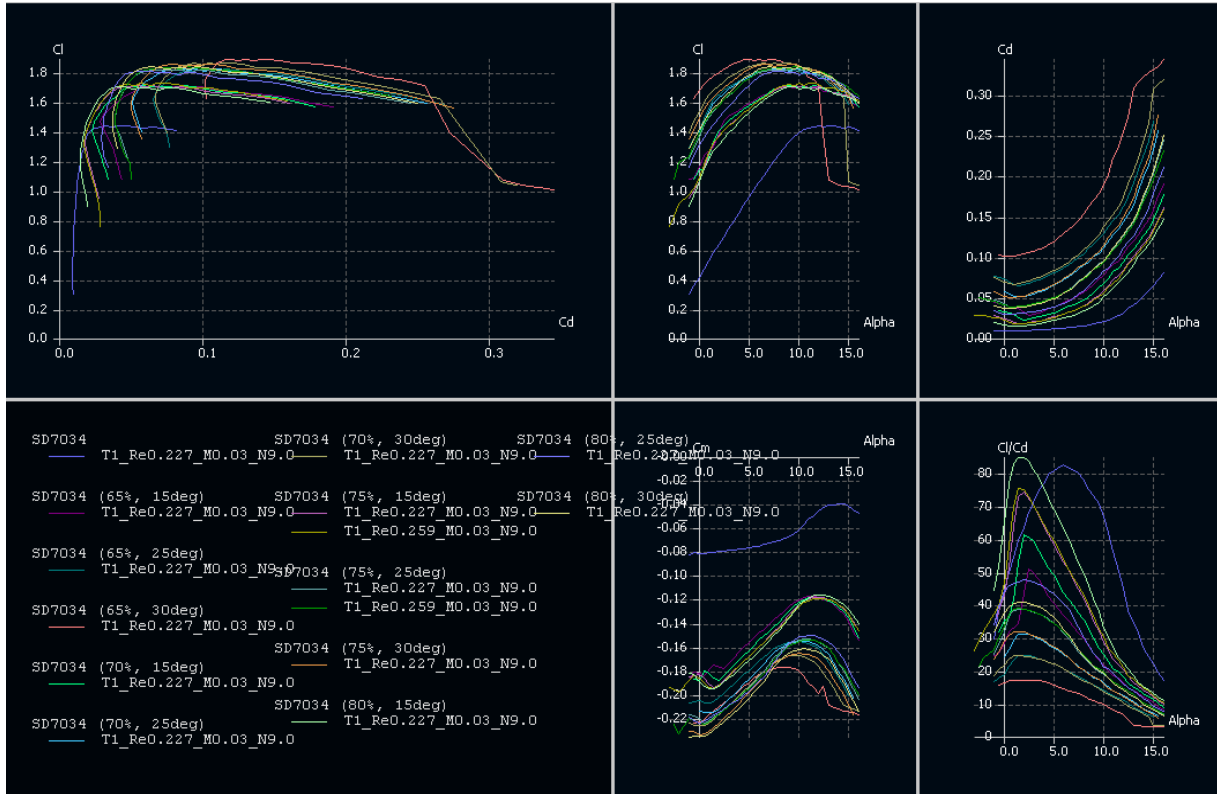


Figure 11: Graphs of different flapped SD7034

DETAILED CFD WING ANALYSIS

With this initial sizing complete, a wing model was created in XFLR5. This was done by modeling the inboard and outboard sections by panel method in the wing creation software of the program. Special consideration had to be made to center the wing at the aerodynamic center for the software to produce correct results. The model was then run at the Reynolds numbers for takeoff and cruise which were described earlier.

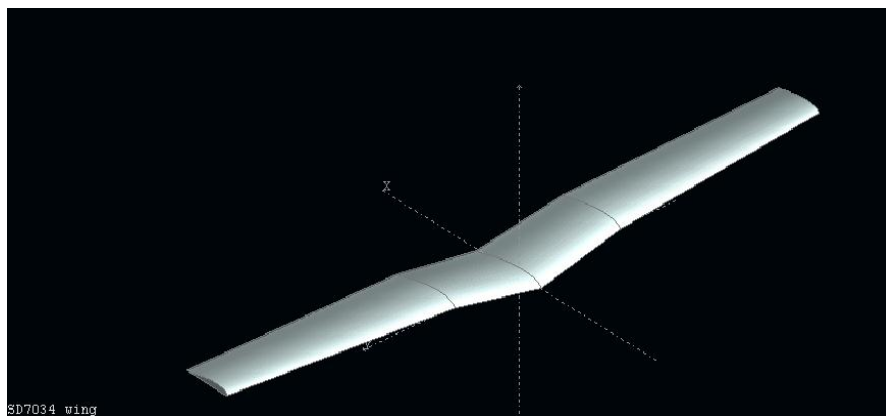


Figure 12: Render of the wing

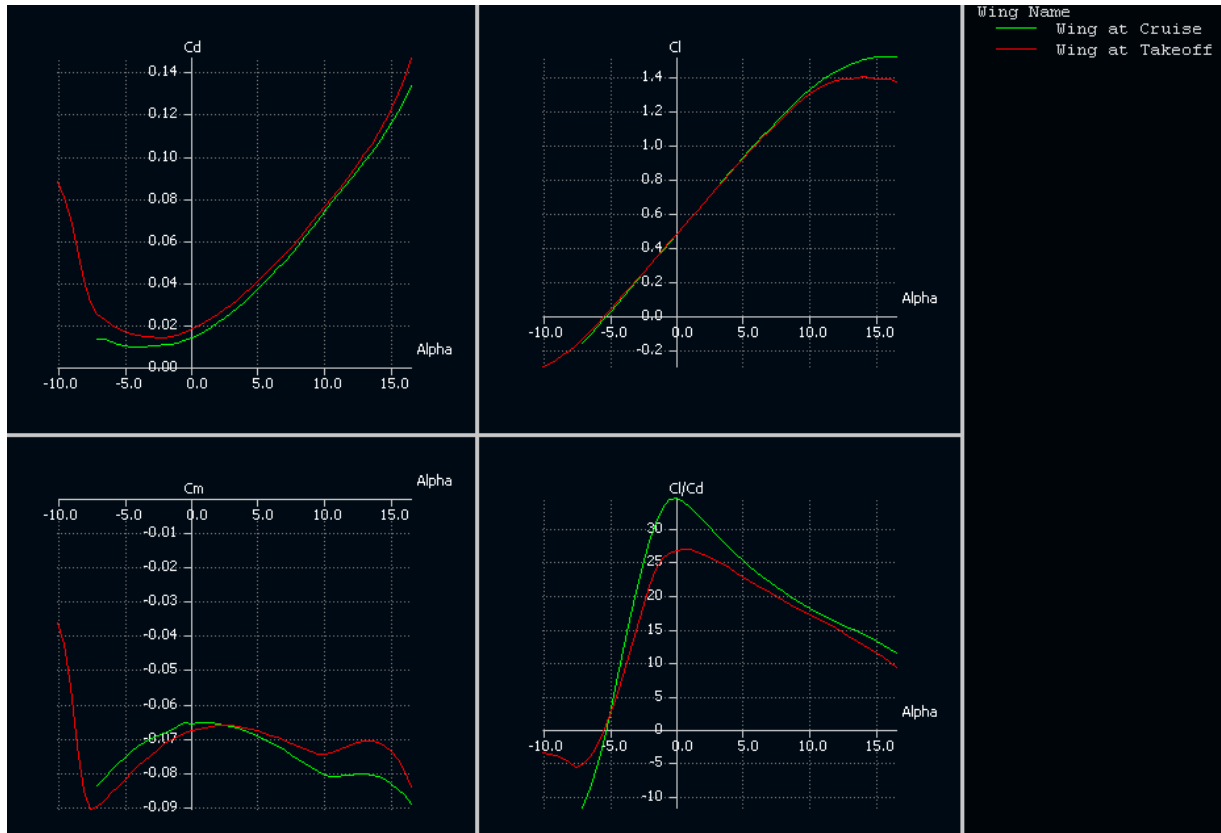


Figure 13: Wing at cruise (Green) and takeoff (Red)

Additional wings were created to model the effects of flaps and flaperons on the wing at takeoff. Results with flaps displayed poor convergence properties, but indicate the desired results. Data for the flaperons was generated and found to give an increase in C_L while not producing an incredible increase in drag.

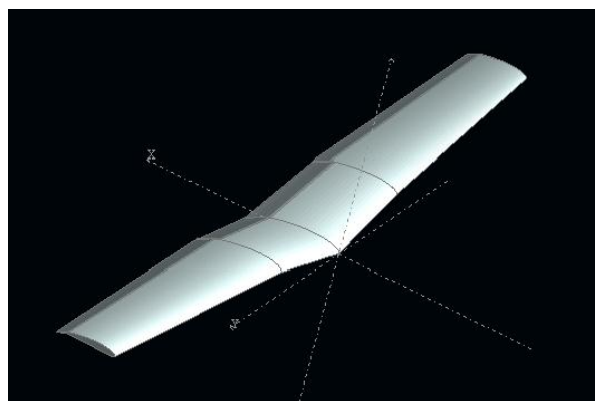


Figure 14: Render of the flaperons

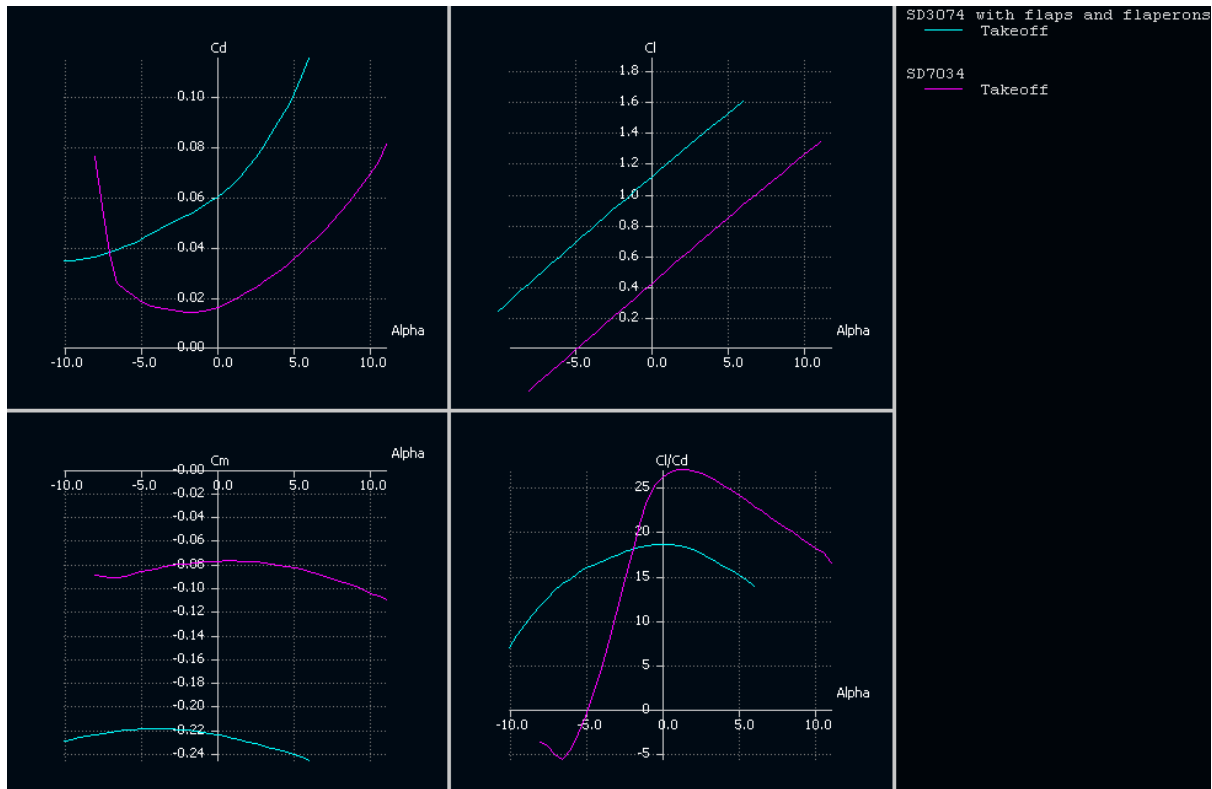


Figure 15: Comparison of normal wing (Purple) and flaperons (Blue) at takeoff

WINGLET CONSIDERATION

Initial research indicated that winglets could potentially improve performance without increased wingspan. Our desired winglets would have been on the bottom of the wing, and used to house small wheels to support the wing tips. However, inflow occurs on the top and bottom of the wing, as well as from bottom to top. Thus, a larger effect is achieved with winglet on top. Disadvantages also include increased drag in some conditions (since the winglet can only be idealized for one regime), and most importantly, higher tip loading, increasing the chance of tip stall. Also, in our application, winglets would move the CLA forward. Thus, they were removed from our design.

TAIL PRELIMINARY DESIGN AND STABILITY

To begin sizing the empennage, a process to evaluate the static stability of the aircraft was undertaken. First, wing moment coefficient C_M was calculated (again, for all regimes). Initially, center of gravity (CG) location was estimated at around 1/3 MAC based on Lennon. Using these values, the wing geometry, and the vehicle weight, the

total negative moment on the airframe was found. The horizontal area and control arm of the inverted V-tail, along with decalage (difference between wing and tail incidence) and control deflection, must always be sufficient to counter this moment.

Simultaneously, the V-tail must serve as a sufficient rudder to maintain directional and spiral stability. This was determined based on Lennon’s method of estimating center of lateral area. Locating the CLA at 25% of the vertical tail moment arm (VTMA) should produce acceptable traits in both stability modes. Initial estimates of tail size were input based on existing aircraft examples, and were quickly refined to produce necessary values.

The following initial tail variables were input: Root chord, taper ratio, horizontal projected span (dependent on boom spacing determined by inner wing panels), sweep, v-angle, tail distance from wing, and decalage. Geometry allowed these values to produce tail areas (projected to both vertical and horizontal), actual panel area, aspect ratio, MAC and AC. With the Reynolds numbers for these surfaces in each regime, and considering the α of the wing in each, the actual countering moment due to the tail was found, along with the estimated CLA. This information allowed more accurate calculation of the CG location, by calculating the neutral point. Two equations were used for this and compared, one from Lennon and one from Simons (not listed here, the calculation is very lengthy and best handled by the spreadsheet). A desired static margin of 15% then yielded an accurate CG location. Reiterating through this process helped optimize empennage dimensions. The required lift coefficient from the tail in each regime was the most important output of this process, since it was required to produce a positive pitching moment exactly equal to the existing negative moment. See ATS Tables 5 and 6.

Stability Design							
(for above regimes and alphas)							
SD7034	Cm	-0.132	-0.0795	-0.075	-0.0775	-0.0792	-0.08
CM Tot		-0.132687	-0.079738	-0.075221	-0.077726	-0.079447	-0.0802405
M Section (ft*lb)		-0.336207	-0.334519	-0.559327	-0.956907	-1.442252	-2.4117854
Mwing Tot (ft*lb)		-1.341452		-3.032467		-7.708076	
Moment due to CG (ft*lb)			-3.100943				
Total negative moments (ft*lb)		-4.442395		-6.133409		-10.80902	
Stability Design (Continued)							
NP Location (Based on wing/tail geometry)				(Should be approx. .35 MAC - Lennon)			
Based on "Model Aircraft Aerodynamics" Martin Simons				Lennon est: (in from LE) 4.656588			
NP (in behind LE)	Static Margin			CG dist from LE (in)			
-5.24238533	0.15			-3.2467			
Vs Stabilizer Volume Coeff	0.617232			(typical below)			
Ns Stabilizer Efficiency	de / da						

Table 5

Advanced Tail Design												
Projected Horiz. Dimensions Half												
Root Chord (in)	Taper ratio	Tip Chord (in)	Span (in)	S (in ²)	AR	Sweep (in)	Tail angle	Actual length (in)	MAC	MAC loc (spanwise, in)	Sweep dist at MAC	
12	0.6	7.2	17	163.2	1.770833	-6	35	20.753168	9.8	7.79166667	-2.75	
(ft)	Tau		(ft)	(ft ²)	1.770833					Along actual length		
1	0.06		1.416667	1.133333						9.511868671		
??												
Projected Vert. Dimensions												
Root Chord (in)	Taper ratio	Tip Chord (in)	Span (in)	S (in ²)	AR	Sweep (in)	Tail angle	Actual length (in)	MAC	MAC loc (spanwise, in)	Sweep dist at MAC	
12	0.6	7.2	11.90353	114.2739	1.239951	-6	35	20.753168	9.8	5.455783735	-2.75	
(ft)	Tau		(ft)	(ft ²)	1.239951					Along actual length		
1	0.06		0.991961	0.793569						9.511868671		
Regimes												
	Takeoff (flaps)	Maneuvering	Cruise	Sprint								
Speed (knots)	18.68	32	50	65								
Speed (mph)	21.496384	36.82464	57.5385	74.80005								
(ft/s)	31.528029	54.00947	84.3898	109.70674								
Weight (oz)	18	18	18	18								
Mach	0.03	0.05	0.08	0.10								
Re Tot MAC	1.56E+05	2.67E+05	4.17E+05	5.43E+05								
Re tip	1.15E+05	1.96E+05	3.07E+05	3.99E+05								
Tail to wing incidence (degrees, i) -2 Called longitudinal dihedral, or decalage (Neglect downwash, minimal) Thus, Wing incidence angle (degrees) 2												
SD 8020	CI/a	0.102 (deg)	Max a (deg)	10								
Tail a to airstream 6.09622 -0.1201 -3.6811												
	CI	0.621814	-0.012249	-0.375473								
	CL	0.566805	-0.012273	-0.398847								
	L tail (lb)	1.746799	-0.110993	-8.806466								
	L tail vert (lb)	1.430894	-0.09092	-7.213835								
From visualizer:	Wing AC distance to Tail AC (in)	-49.886										
	Mtail Tot (ft*lb)	-5.948464	0.377971	29.98911	(Match to other moments)							
Elevator deflection required?												
(Tot)	L tail vert needed:	-1.068611	-1.475382	-2.600093								
	L tail needed:	-1.304533	-1.801109	-3.174127								
	CL needed:	-0.423298	-0.199152	-0.143757								
	CI needed:	-0.397065	-0.193148	-0.140602								
SD 8020	Elev. Deflection (deg)											
Elev. Try at 70% chord		25	3	-3.5								

Table 6

Control deflections were also considered, since for each regime, some trim was still needed to achieve needed moment. As discussed in Airfoil Selection, the low drag SD8020 was already selected for the tail. Optimizing control surface location as for the flaps, an XFLR5 database was compiled with lift and drag coefficients for a range of surface deflections in each flight regime. Cross-referencing this to the calculated necessary lift coefficients, the necessary deflection for each condition was determined, and more adjustments were made to keep these deflections within acceptable ranges. No more than 25 degrees elevator deflection should be necessary, even to hold the aircraft just above stall speed, but the design is built to allow 30 degrees to ensure adequate control at all times.

With pitch control and longitudinal stability well optimized, the directional stability was still less than desired. To correct this, one option was to make the angle of the v-tail steeper, but this created a much larger surface than necessary for pitch control with excess drag. Instead, “vertical surface augmentation” was added in the form of two small, entirely vertical horizontal surfaces under each boom. These increased the lateral area at the rear of the aircraft and brought the CLA to the desired 25%. See ATS Table 7.

Directional/Spiral Stability (Vertical Tail Design)																
Est Lateral Fuselage Dimensions:											Centroid x	Centroid y				
Top Length (in)	Bottom Length (in)	Height (in)	Sweep to bottom front (in)	Nose dist from LE (in)					from LE (in)	from root (in)						
40	20	5	10	150	20					0	-2.22222222					
Vertical Surface Augmentatio (under boom)																
Projected Vert. Dimensions											Centroid x	Centroid y				
Root Chord (in)	Taper ratio	Tip Chord (in)	Span (in)	S (in ²)	AR	Sweep (in)					MAC	MAC loc (spanwise, in)	Sweep dist at MAC	LE Dist A from LE (in)	from root (in)	
12	0.5	6	4	36	0.444444	7					9.33333333	1.77777778	3.111111	0.777778	47.777778	1.222222
Winglets (canceled)																
CLA x from LE (in)	CLA y from root (in)	VTMA (in)	SSM (in)	CLA (% VTMA)	(aka SSM as %)											
13.8072482	3.0208584	41.93516	10.54241	25.1398	(Aim for 25%, Lennon)											

Table 7

Finally, the trim drag due to the empennage was estimated, again using general drag equations and estimation techniques (as for the wing), total drag due to the v-tail was calculated. See ATS Table 8.

Tail + Trim Drag Calculations				
(for above regimes and alphas)				
SD8020	Cd	0.054	0.0085	0.008
	d	0.2	0.3	0.3
	e	0.833333	0.769231	0.769231 (p.428)
	Cdi	0.048921	0.011771	0.006157
	CD Tot	0.102921	0.020271	0.014157 (Equation from Anderson p.430)
	D tail Tot (lb)	0.31718	0.18333	0.31258 (Equation from Anderson p.432)
	Actual wing+tail L/D	8.52677	19.314	16.1977

Table 8

DOWNWASH

It may be noticeable that downwash angle from the wing is not considered in the analysis. This is because due to the opposite dihedral angles of the tail and the inner wing section, minimal to no down wash from the wing passes over the tail. This will be seen further in the CFD analysis.

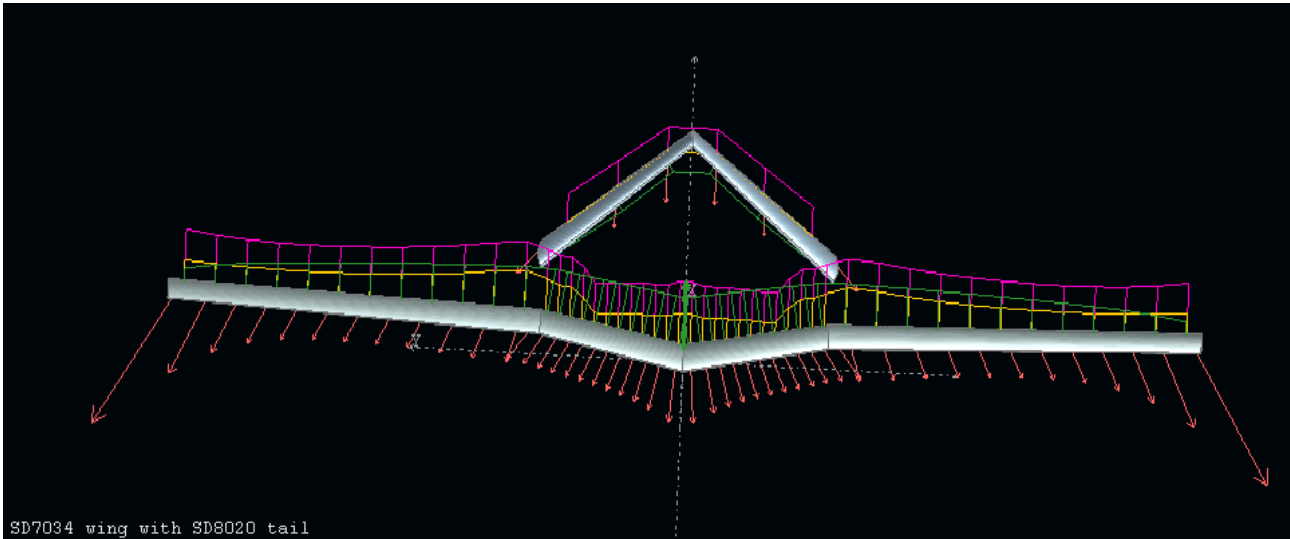


Figure 16: Downwash Example

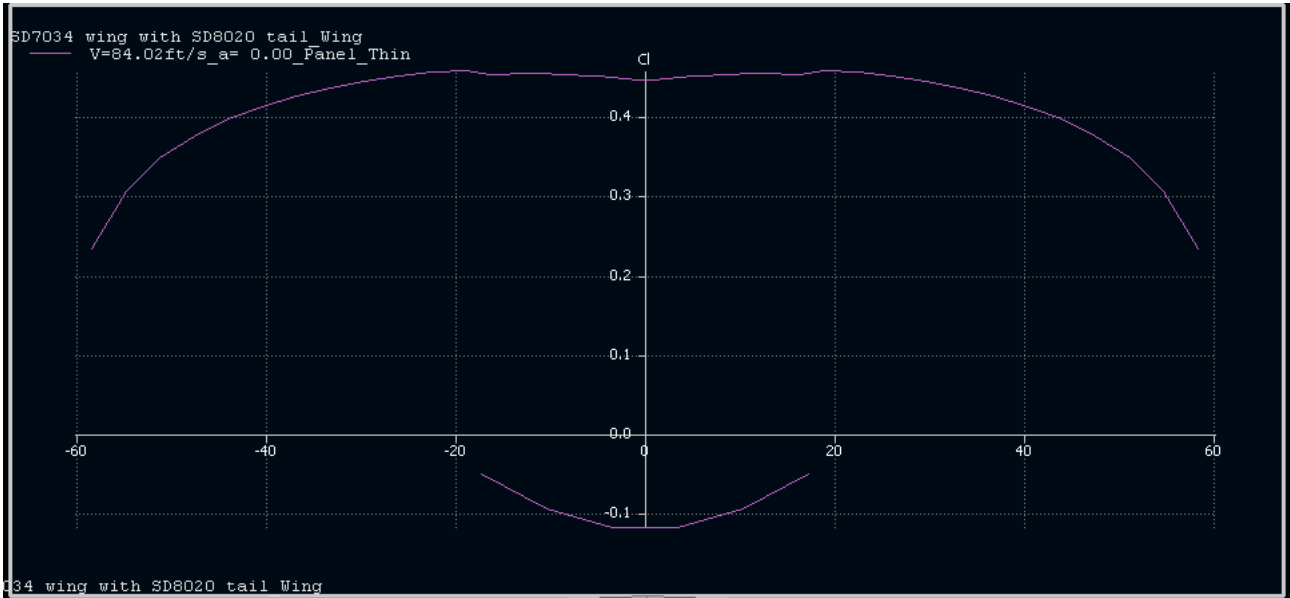


Figure 17: Lift Distribution of wing and tail at cruise

DETAILED CFD TAIL ANALYSIS

Now the entire aircraft could be modeled in XFLR5. The tail was modeled in conjunction with the wing so that their effects on one another could be analyzed. The largest effect shown in the new analysis was the stability of the wing with the addition of the tail. This can be seen in XFLR Figure 19, where it is clear that the inclusion of the tail gives the C_M slope a constantly negative slope. The L/D also saw a decrease along with slightly increased C_D .

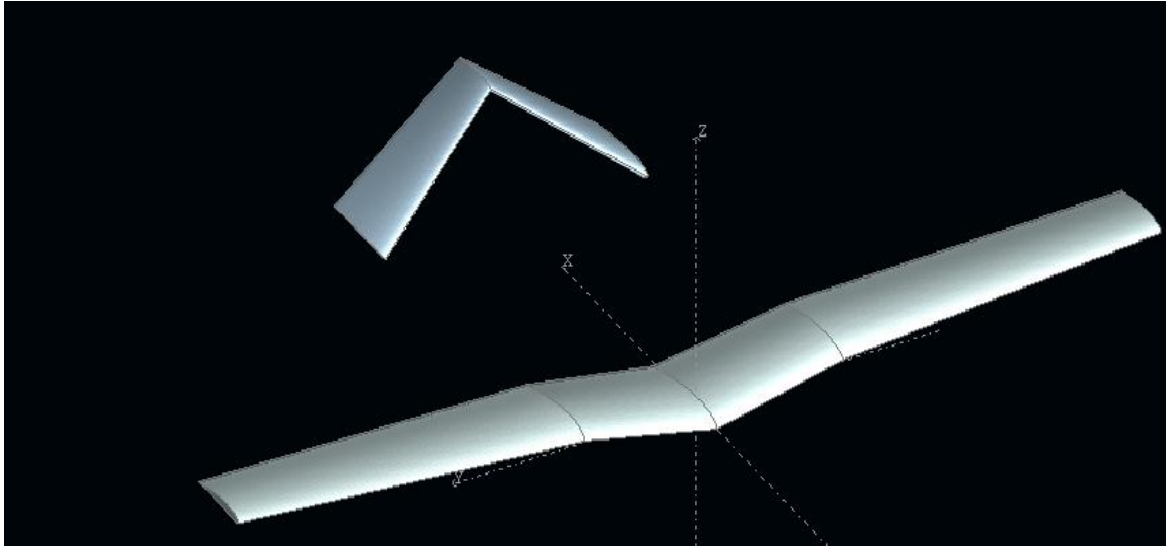


Figure 18: Render of wing with tail

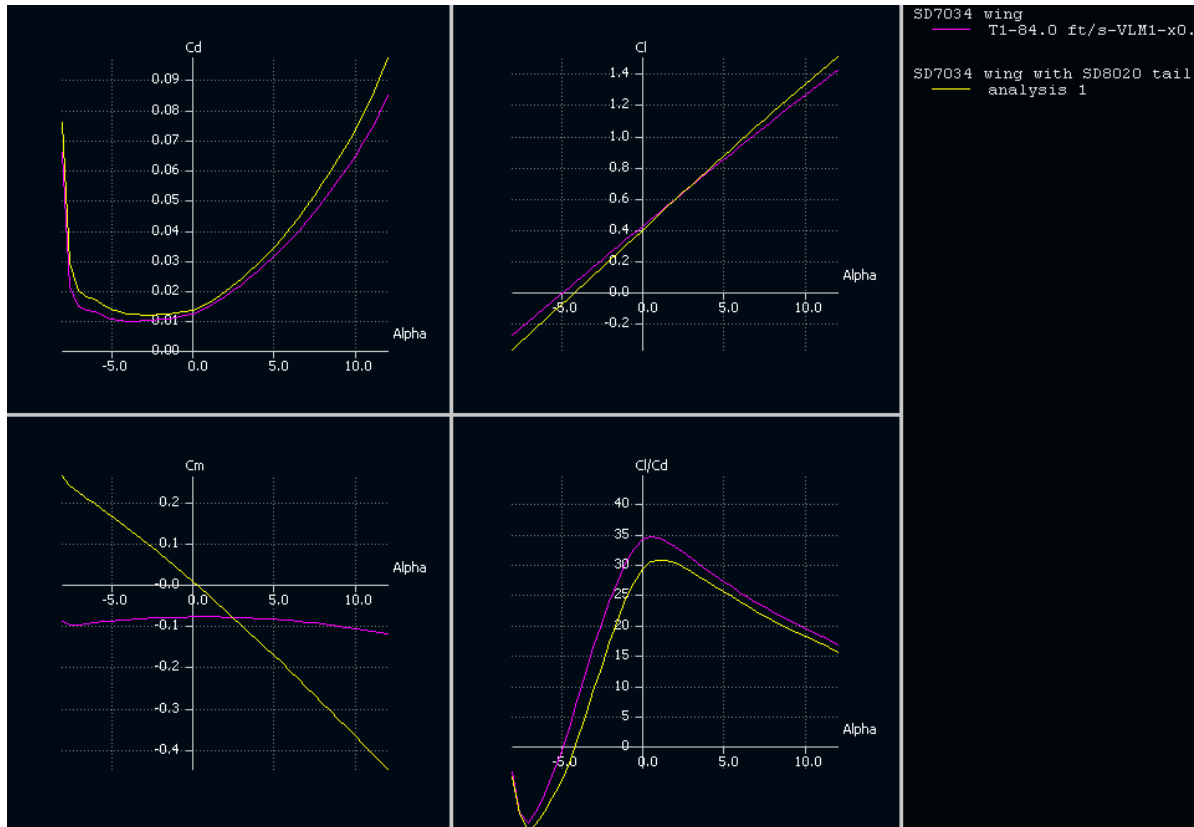


Figure 19: Comparison of wing (purple) vs wing with tail (yellow)

INCREASED AIRCRAFT WEIGHT CONSIDERATION

Many aircraft end up heavier when constructed than designed. With this consideration in mind, the spreadsheet was also run with the weight at 30 pounds. Takeoff was still easily achieved by increasing the takeoff speed from 20 to 25 knots. This result was confirmed by XFLR5 as well.

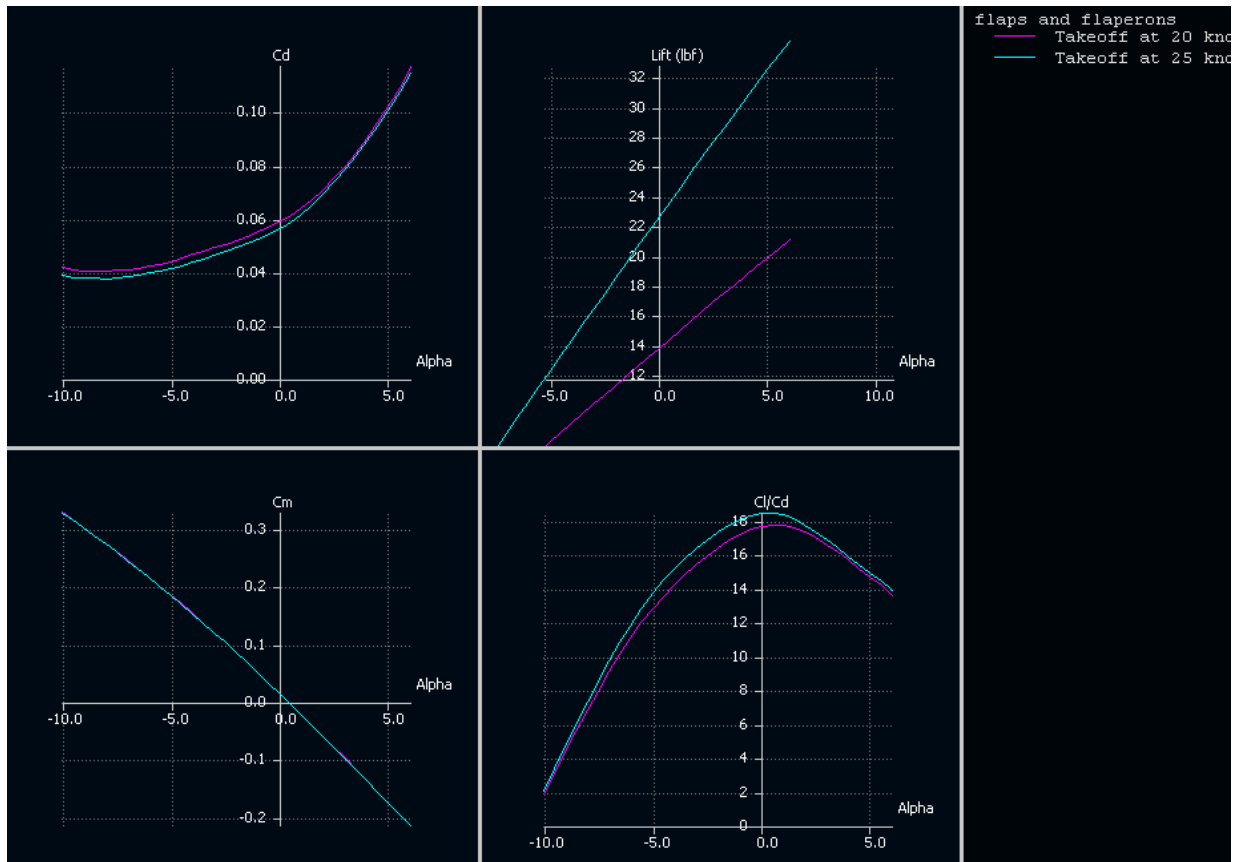


Figure 20: Weight comparison from 20 to 25 knots

XFLR5 was also run with the fuselage included to confirm and augment the final performance values. The lift and drag data with fuselage included is displayed in the figure below. The final figure in the CFD analysis displays the pressure distribution across the major components of the aircraft. The results obtained from these figures are reported in subsequent sections.

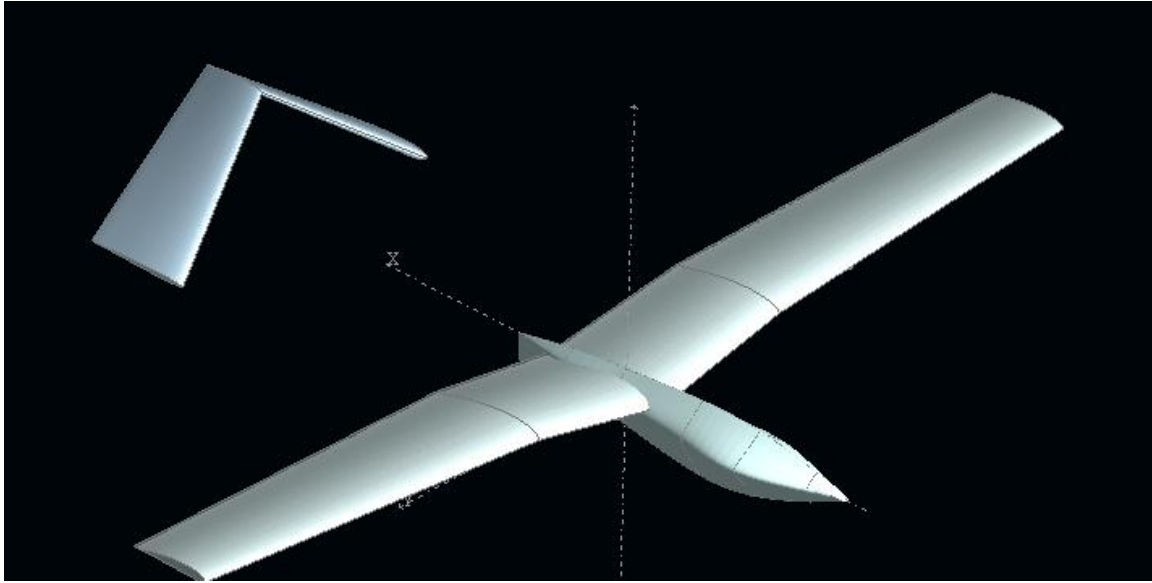


Figure 21: Fuselage included

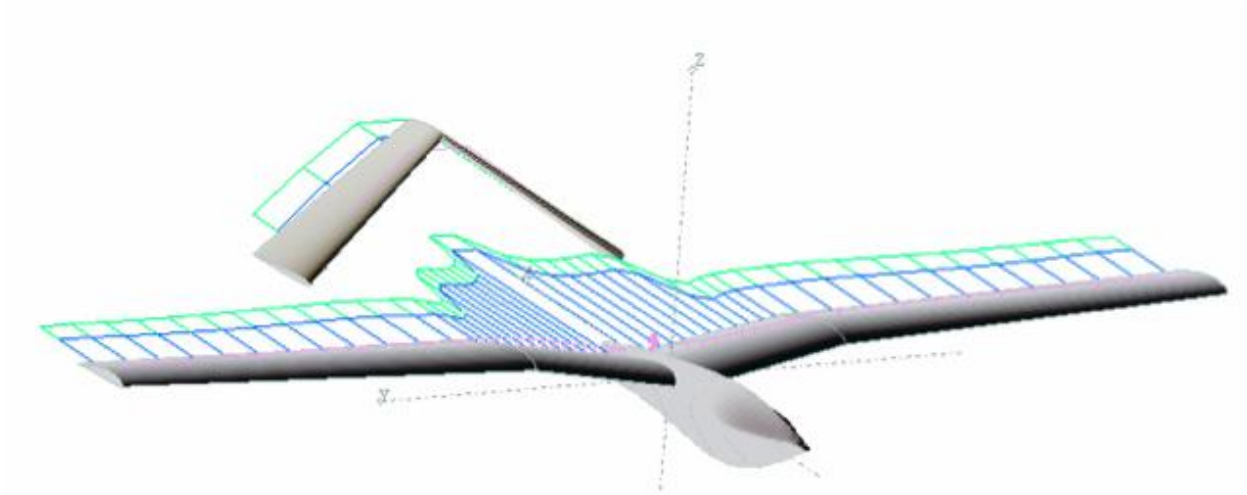


Figure 22: Lift and Drag Analysis

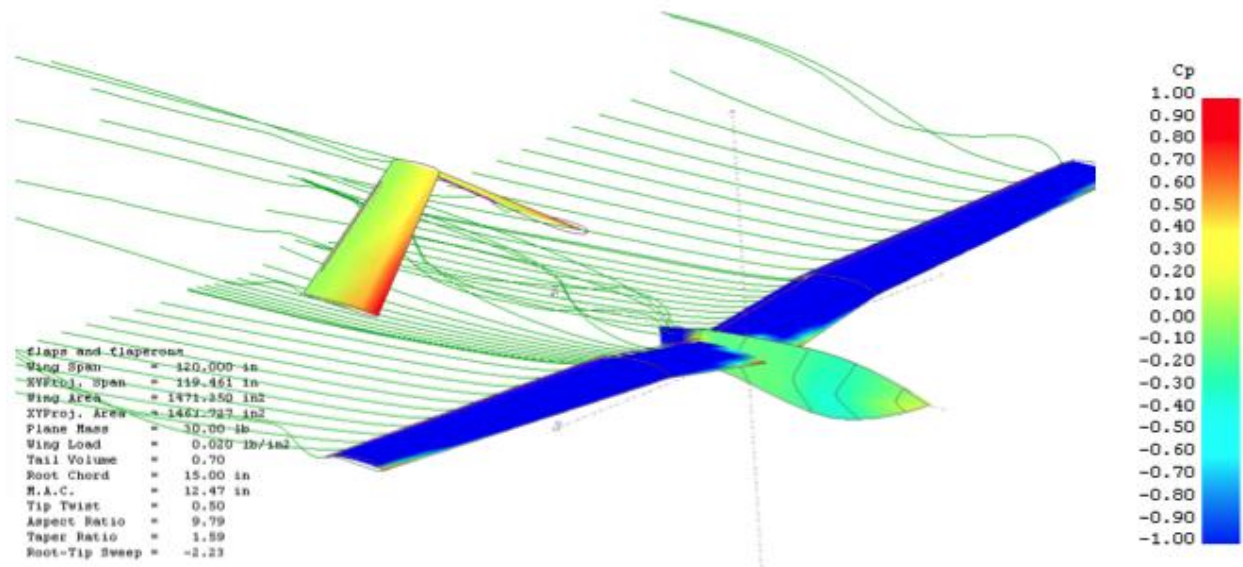


Figure 23: Pressure Distribution and Streamline Analysis

CAD MODELING

After design steps were near finalized, the entire vehicle was modeled in SolidWorks. Each part was modeled exactly, with appropriate mass properties/density, and assembled into the entire final aircraft. Renderings of this model are used throughout this report. The model was also used to calculate and adjust the location of major components to precisely place the center of gravity. It will be used to create the actual molds to manufacture the AVATAR, and for reference during construction. Exact drawings of every component and structure in the vehicle can be produced instantly from this model. More SolidWorks renders are also included in the appendices.

FUSELAGE DESIGN

The fuselage design is one of the most important parts of the project, due to the fact that it houses all the equipment that will come from the interdisciplinary design team. The fuselage needs to be able to contain all the hardware they require for the system to function, as well as the hardware needed to fly the plane (autopilot, etc.), therefore the fuselage went through a range of changes until the design was finalized.

THE EVOLUTION OF THE FUSELAGE

The first design was made to fit everything into top and bottom sections. The top part was mainly for the hardware that the plane requires in order to fly manually, therefore a relatively small space was needed. The bottom part was for the entire

payload components required for the camera system to work plus the autopilot interface; therefore it needed a large amount of space. The leading edge of the bottom shell was clear so the camera could look out. No landing gear was incorporated at this stage in the design.

Changes in the design were progressively implemented. The first major variation was increasing the capacity of the upper payload portion, as it was realized that a large volume would be needed to store flight batteries. Similarly, the next fuselage revision was able to be open from the top, which gave easier access to all the hardware and eliminated the problem of having to remove the whole bottom half to work on any of the internals. Another change was that the top and bottom were now fused into one piece. Even though they were unified, there would still be a removable portion for the camera hardware and another bay for the normal flying hardware. One final change (prompted by the interdisciplinary team) was the inclusion of a dome for the camera to see through; this made the distortion of light passing through the dome independent of direction because of the uniform curvature and thickness of the dome. Since the bottom of the fuselage would almost be completely removable and would cause strength problem when landing, the landing method was still unclear.

The final design changes were made in order to strengthen the fuselage and include a landing method. In the third design it seemed that there would be strength problems because most of the top and the bottom of the fuselage had large removable sections. The bottom of the fuselage would only contain a cutout hole that in order to fit the dome for the camera and small landing gear slots. The opening on the top would be separated into two different compartments; the one in the front will be for a special holding grid that can be removed. The grid will be used for the camera hardware, so if needed the whole section can be lifted out in order to work on its contents. The compartment in the back of the fuselage will be used for the regular hardware that is required for flight. Due to the weight of the plane, the landing method chosen was fixed landing gear. Since the bottom of the fuselage was strengthened and no longer separable from the top, fixed landing gear was implemented. To minimize drag, a bicycle landing gear setup was employed, with small stabilizing outrigger wheels to prevent tipping from side to side. Properly designed fuselage formers and shock absorbing hardpoint blocks allow for traditional tricycle landing gear to be mounted. This will probably be the configuration of choice for early test models, and the move to bicycle landing gear will be made later if possible.

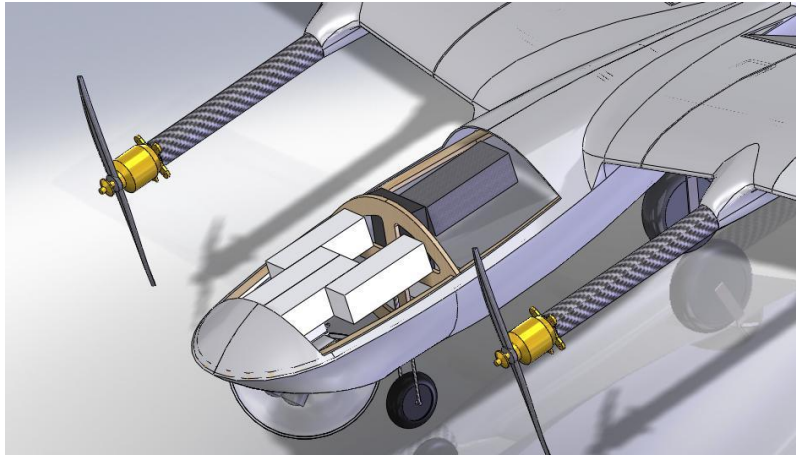


Figure 24: Fuselage with top skin removed

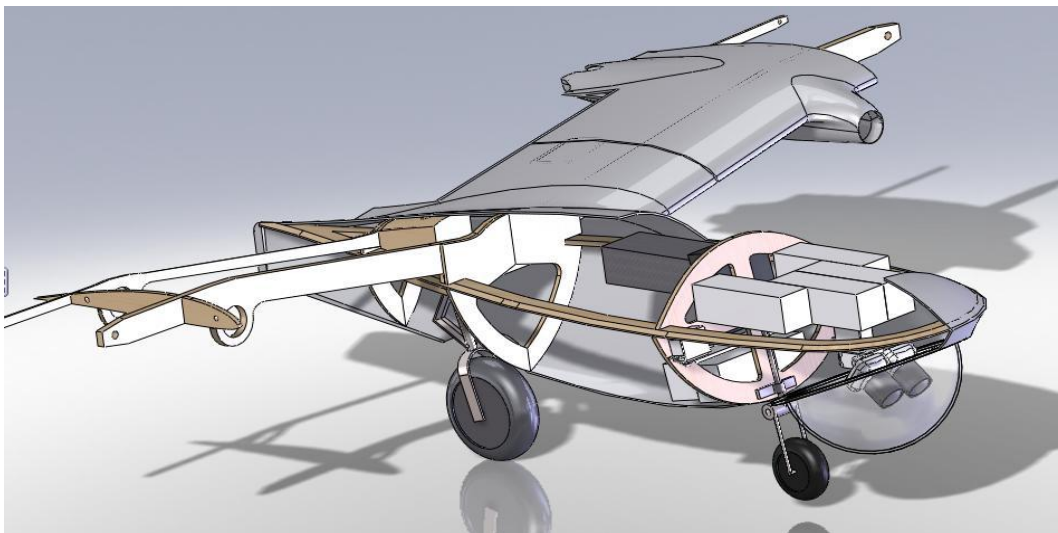


Figure 25: Internal structure of fuselage structure

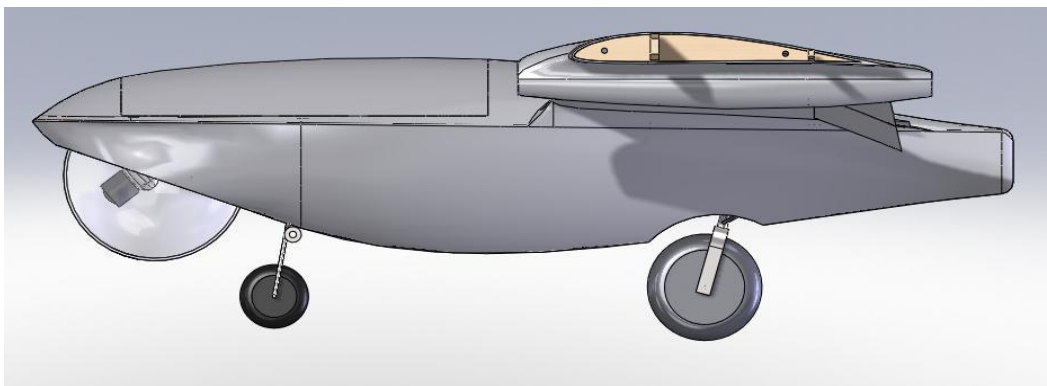


Figure 26: Fuselage Side View

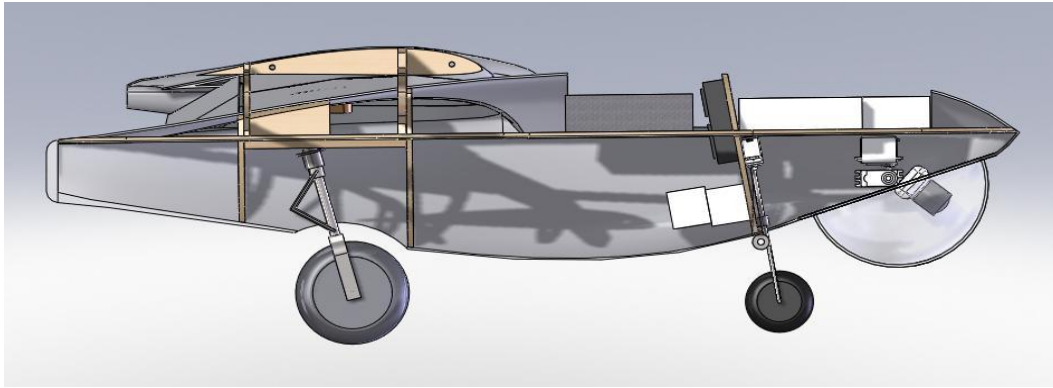


Figure 27: Fuselage Internal Structure - Side View

FUSELAGE CFD ANALYSIS

Analysis for the shape of the fuselage was done with XFLR5. A variety of airfoils were tested and an acceptable shape was chosen based on acceptable capacity, minimal drag, and minimal flow separation. See Figures 29 and 30.

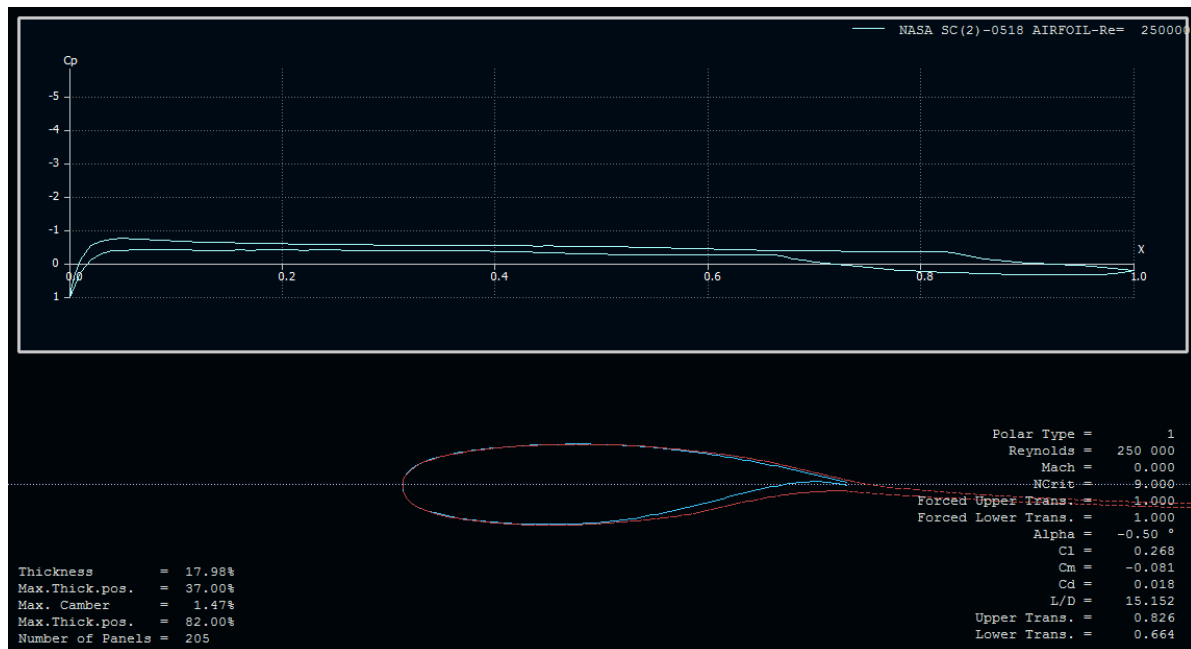


Figure 28: Showing the separation of the flow at 0° angle of attack.

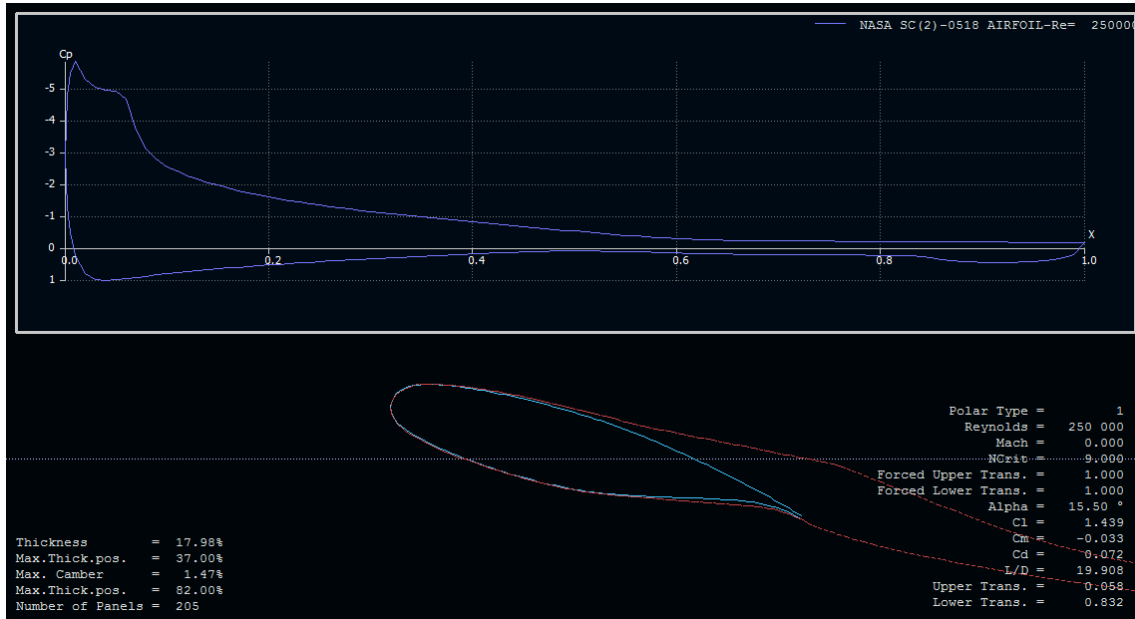


Figure 29: Showing the separation of the flow at 15° angle of attack.

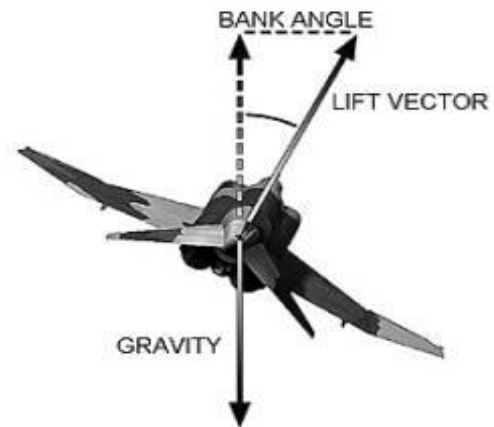
PERFORMANCE ANALYSIS

TURNING ANALYSIS

In order to optimize the flight path for the competition, it is critical to know the turning characteristics of the aircraft at different speeds. In order to do this, a turning analysis calculator was developed in an excel spreadsheet. This calculator determines the loading factor, turning rate, turning radius, and turning time for inputs of flight speed and bank angle using the main equations presented below.

$$R_{turn} = \frac{V^2}{g \times \tan(q)}$$

$$Time = \frac{2\rho \times V}{g \times \tan(q)}$$



Turning Analysis (level turning flight)

Cruise Speed	50 (knots)	57.5385 (mph)
Load Factor	1.31 (G Load)	
Bank Angle	60 (MAX)	
Stall Speed	18	

Turn Rate:	Turning Radius	Turning Times (sec)	Increased Stall Speed
0.32 rad/s	128.5 ft	9.5 (360 deg)	1.4 (Factor)
18.3 deg/s	Turning Diameter	4.8 (180 deg)	25 KTS
	257 ft	2.4 (90 deg)	

TEST PLAN

The first stage of testing will involve bringing the plane to preflight readiness and perform a high-speed taxi test. This will ensure that all the equipment works properly. Another major component considered for the first stage is simulation tests using an AVL model to prepare for autopilot testing in the future. AVL or Athena Vortex Lattice is a simulation model which allows for accurate analysis of aircraft configurations. The AVL model is shown below:

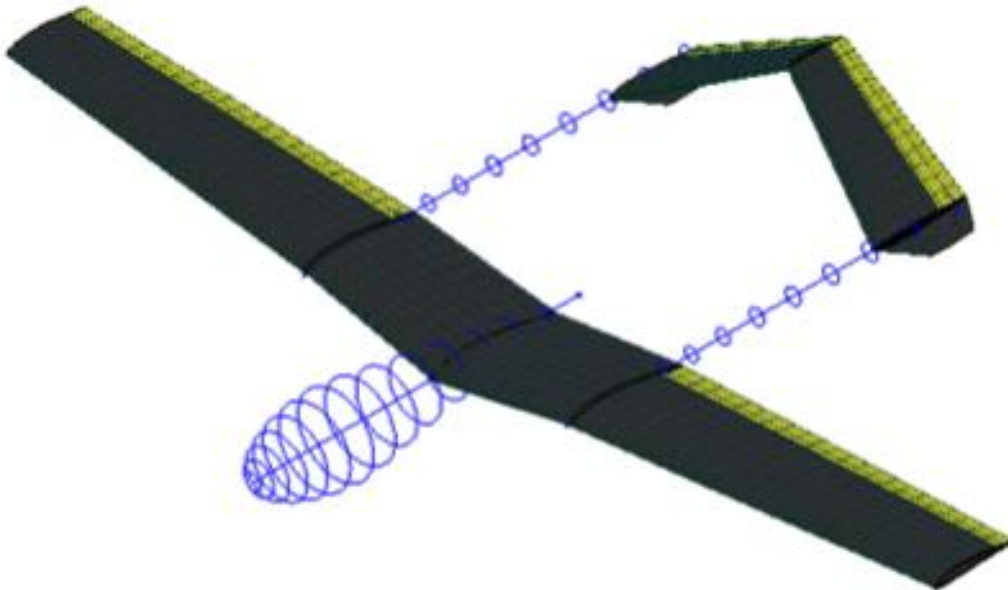


Figure 30: AVL Simulation Model

The second stage of testing will consist of several test flights. The first set of flights will be short, with a minimum payload of batteries to allow the pilot to become comfortable flying the aircraft and measure power drain on the batteries. The second set of flights will simulate a full payload allowing observations of the mission profile.

The third stage will focus on autopilot integration and testing. After the initial simulation from the first stage, the autopilot will be tested with a minimum payload. As the team's experience and confidence with the autopilot increases, simulations will begin to include the full payload of the aircraft. This will include early tests of aerial photography, and eventually autonomous takeoffs and landings.

The final stage of testing will be the complete simulation of the mission plan. This will allow the team to make final preparations for the competition and run through the entire mission profile.

At this phase in the design the first stage of testing has already been completed. The aircraft performed a successful taxi test and the AVL simulation

BILL OF MATERIALS

See Appendix B for the Bill of Materials

MANUFACTURING CONSIDERATIONS

Multiple manufacturing methods have been considered for the construction of the airframe, some more desirable than others. Below is a list of the manufacturing methods that were considered for the separate components of the aircraft.

FUSELAGE AND INBOARD WINGS

- **Mold Design** – Molds will be designed and built based on CAD design of airframe and the airframe skin and internal structure will be set within the pressed mold. Internals will be made out of composite materials (carbon fiber or fiber glass/plywood)

The mold method is preferable due to the complicated design of the fuselage. This method is also easier to implement and maintain the integrity than other methods. The

internal structure can most easily be assembled through this method while maintaining the correct surface according to the CAD design. The only disadvantages of this method are cost and time of construction, but being the most important component it is necessary to make a mold for the fuselage.

OUTBOARD WINGS

- Mold Design - Molds may be designed and built based on CAD design, in a method similar to that of the fuselage (if budget permits).
- Foam Core Stencil - Stencil is manufactured through CNC and foam will be hot wire cut along shape of stencil. Foam core will be covered in composite skin (using leftover foam chocks as a one-use mold) and hollowed out to fit internal structure.

The mold method is once again preferable however it is not as imperative to employ as in the case of the fuselage design. In the interest of time and cost the team is willing to implement the foam core stencil method if necessary. The outboard wings are much less complicated than the fuselage and the tail and therefore if there is insufficient funding for all the required molds this component will be the first to undergo construction through an alternative.

TAIL

- Mold Design - Molds will be designed and built based on CAD in a method similar to that of the fuselage.
- Foam Core Stencil - This method could potentially be employed again if budget does not permit mold manufacture, though complex curvature makes foam coring more difficult.

Once again the mold method is the most desirable especially due to the complicated design of the tail. If a mold cannot be implemented a foam core stencil method will be the preferred alternative.

LANDING GEAR

The landing gear will be mostly internalized. Off-the-shelf nose and main struts and wheels will be purchased and assembled. These will mount into plywood/carbon hard-points in the structure designed to transfer landing loads into the spars and other aircraft structures. The vehicle is currently designed to employ bicycle landing gear with supporting outrigger wheels, but if this is later deemed unappealing, the same

hard-points have been located to allow regular tricycle landing gear to be installed while utilizing the same nose gear.

MATERIALS AND PARTS

In each of the above components the skin will be constructed out of fiberglass with an AEROMAT core. The internal structures will be constructed out of plywood or balsa and carbon fiber fabric or fiberglass depending on price and weight and the booms will be made out of carbon fiber tubes. The specific materials and parts to be used are compiled in the subsequent section.

COMPOSITE CONSTRUCTION

MOLDS

After taking the considerations discussed in the previous section it was decided to utilize molds in the building process of the tail. Construction of the molds was a lengthy process that entailed generating G-code from the CAD model in order to machine the 6 lb high density foam to the appropriate shape and applying Duratec Surface Primer to the foam, which then had to be sanded to the appropriate surface finish. Similar to the construction of the components of the aircraft, this is a composite process.

SKIN

Once the molds were created the skin of the fuselage and tail could easily be constructed. With the proper Duratec finish on the molds a coat of dried PVA followed by gelcoat was sprayed onto the surface of each mold. Once the gelcoat has been applied to the mold surface and allowed to dry, layers of composite materials can be placed directly onto the dried gelcoat with epoxy brushed into these layers to create the skin. The lay-up process of the skin was a layer of 2.4-oz/sq. yard fiber glass followed by a 3.6 oz layer, then the AEROMAT core, and finally another layer of 2.4-oz fiber glass. The fiberglass is placed in the lay-up at alternating fiber directions of 90°, 45° and finally 90° again. The alternating direction of fiber strands increases the strength of the finished product. After the appropriate amount of epoxy has been added to each layer a series of extra layers are added before the entire mold is vacuum bagged in order to properly bind each layer as well as drain the excess epoxy. A diagram displaying the composite layers of the skin is shown below:

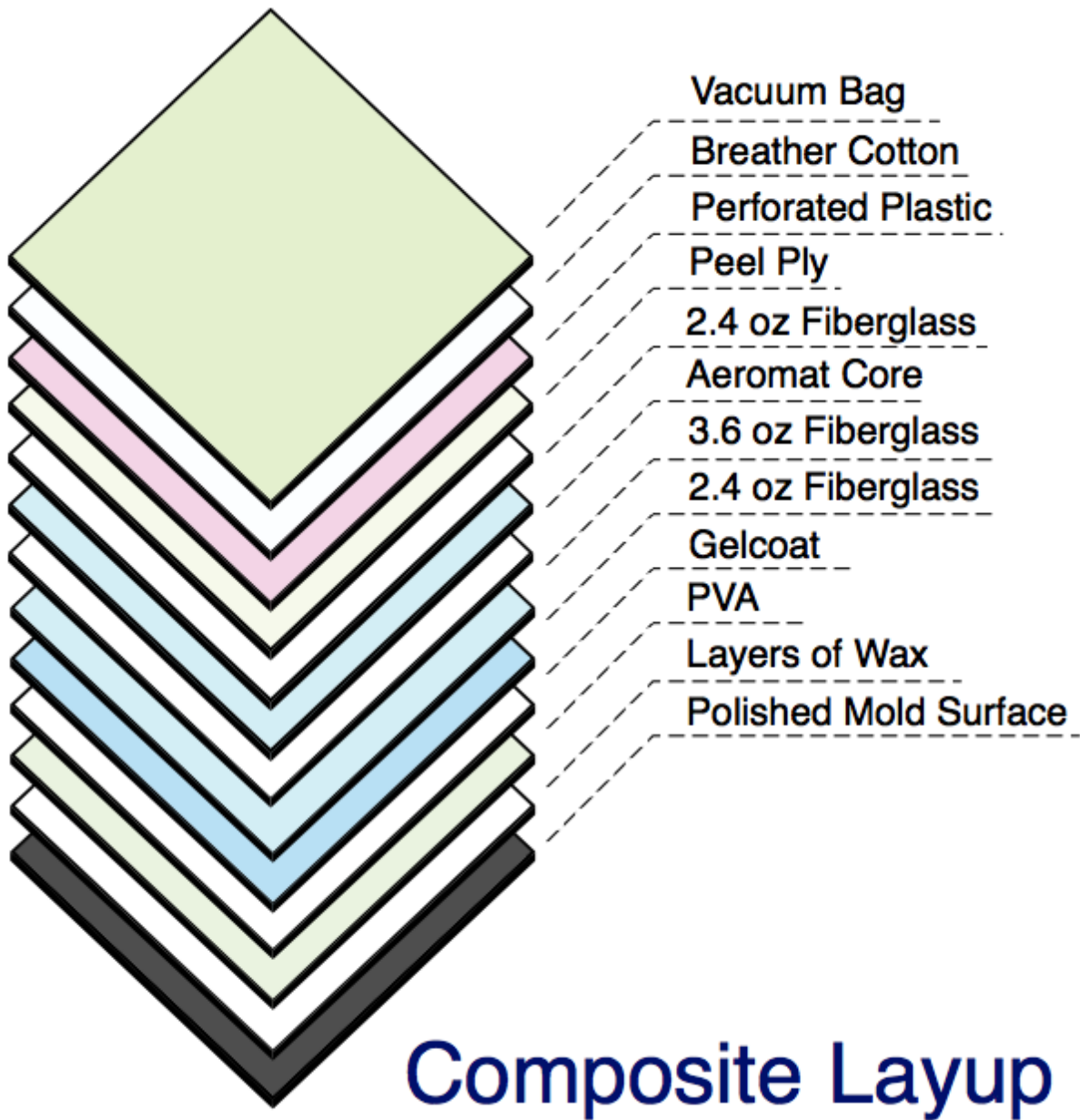


Figure 31: Composite Skin Layers

SPAR AND INTERNALS

The spar is the most important internal structure within the aircraft and as such it required a unique lay-up process that would allow it to remain lightweight, long, but extremely rigid. The main component within the spar was two long pieces of balsa wood with opposing grain direction. Surrounding the balsa are various layers of fiberglass and carbon fiber. The 2.4-oz fiber glass is applied to the front and rear faces of the spar and 0.03" multidirectional carbon tape is applied to the top and bottom of the

spar, two layers on top one on bottom. After these layers are added another layer of 5.8-oz carbon fiber was wrapped around the entire surface of the spar. The diagram below displays the layers of the spar:

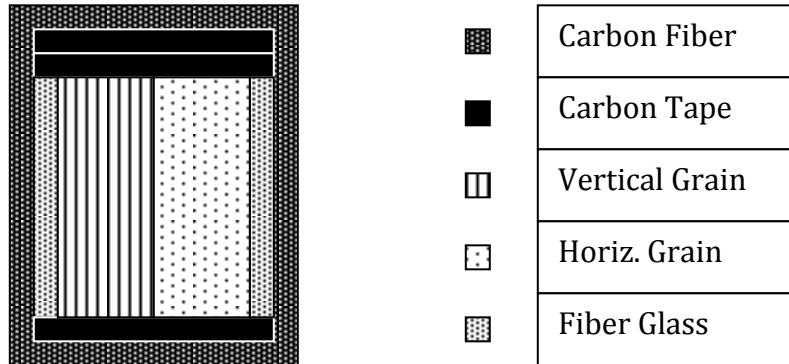


Figure 32: Composite Layers for Spar/Internals

The layers of the rest of the internal were the same as the spar only without the inclusion of any carbon. The reason the internals are not reinforced with carbon is because they do not require the same amount of stiffness, but rather are more important for maintaining the structure. The added weight would be very great if each internal had carbon, which is another reason for the absence.

JOINERS AND OUTBOARD WINGS

As mentioned in the Manufacturing Considerations, outboard wings are a separate component of the overall design and due to this separation telescopic joiners had to be created in order support the structural weak point of separation in the spar. The original design called for forked spars with pins to secure them in place, however in the final construction the carbon tube joiners were found to be a stronger joining method and thus were used in favor of the forks and pins. The joiners consist of carbon tubing set into epoxy mixed with glass micro spheres, which creates a very strong joint. The tubes are then inserted into holes in the outboard spars when fully assembled. The outboard wings were created using a different composite approach described in the Manufacturing Considerations section. Specifically this technique is called the “Remnant Foam Method” in which a foam core is cut out using a hotwire and then 3.6 oz fiber glass is placed between the excess foam or chocks and Mylar. In this case the fiberglass was arranged at a 45° angle.

CURRENT CONFIGURATION

At this phase in the design the aircraft is fully constructed utilizing all of the composite techniques described above. All the control surfaces are in proper working order; however the flaps have yet to be constructed. The flaps will be introduced at a later date in time for the competition. The aircraft will be able to perform full flight tests without the use of flaps as shown in the wing analysis section. As competition approaches the flaps will need to be implemented in order to fully integrate each of the vital systems required for the competition.

PROJECT TIMELINE

Dec 6, 2010 - Jan 9, 2011

Prepare molds/CNC parts for manufacturing. Outsource or begin construction. Complete any necessary conceptual model testing before final construction begins. Order all necessary materials.

Jan 10 - Feb 6, 2011

Complete manufacturing of molds and CNC parts. Construct payload bay for interdisciplinary team's use.

Feb 7 - Mar 6, 2011

Lay-up all composite structures and prepare for assembly.

Mar 7 - April 3, 2011

Assemble aircraft. Integrate electronic components and prepare for flight testing.

April 3 - May 5, 2011

Complete flight-testing and analysis. Make limited improvements where necessary. Prepare final presentation and report.

Summer 2011

Integrate and test autopilot and interdisciplinary team's payload. Test, tune, and prepare for competition.

CONCLUSION/SUMMARY

The objective of this project is to design and construct a UAV with the ability to identify targets, measure the coordinates of said targets, navigate a set flight path, perform the tasks in a set time, and have the ability to re-task. The major goal of our team is to provide the airframe that will carry the equipment produced by the separate interdisciplinary team in order to perform the stated tasks. The final performance results and design values that were chosen for the construction and analysis of the airframe and its components are summarized below:

FINAL FLIGHT PERFORMANCE VALUES

Final Performance Values	
Weights	
Empty weight (lb)	15
Weight with maximum batteries (lb)	22
Maximum payload (lb)	8
Optimal Wing Loading (oz/ft ²)	26.4
Maximum takeoff weight (lb)	30
Designed G loading	+3,-2
Speeds	
Takeoff speed (15 degree flaps) (knots)	20
Takeoff speed (no flaps) (knots)	25
Cruise speed (knots)	45
Stall speed (dirty) (knots)	18
Maneuvering speed (knots)	32
Best L/D speed (knots)	40
Cruise Performance	
Best L/D	24.5
Cruise C _L	0.4
Maximum flight endurance (min)	40
Maximum range (miles)	38
Optimal turn rate (degrees/seconds)	360/19
Service Ceiling (ft)	8000
Power and Control Systems	
Motor (2)	Brushless, 515 rpm/V, 86% efficiency
Electronic Speed Controller (2)	70 amp burst, 55 amp continuous
Operating power (total)	Up to 2000 Watt burst, 1400 Watt continuous
Batteries (5 to 6 packs)	5-6 cell 18.5-22.2V, 25,000 mAh capacity
Control surface actuation	Hitec HS-5685 MH Servos
Servo strength	>150 oz-in of torque at 4.8 volts

FINAL XFLR5 PLOT FOR TOTAL AIRCRAFT

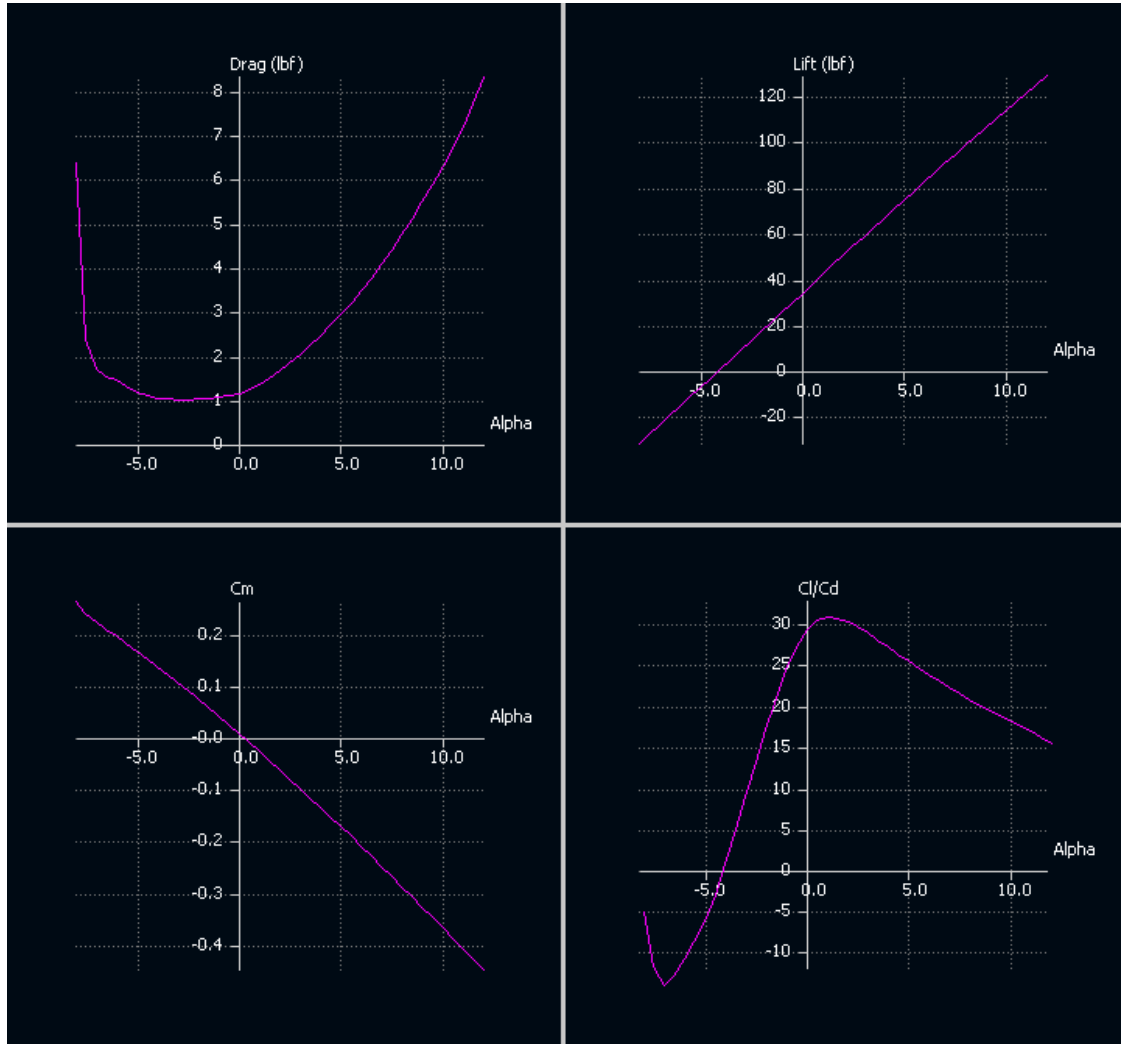


Figure 33: Final XFLR5 Aerodynamic Plots

POWERPLANT

Hacker A50 12S Motors were chosen because they will provide the necessary thrust. They will be implemented in a twin boom configuration in order to provide more thrust but more critically to avoid obstructing the view plane of the camera. Battery power will be provided by 5 to 6 cell lithium polymer batteries with a total of 25,000 mAh capacity.

WEIGHT AND SIZING

The wings and booms are detachable in the interest of transportability. According to planform design the wing loading is appropriate for a short takeoff with the use of flaps. The airframe was designed and strengthened to accommodate varying payloads

with different electronic components and most importantly to allow for an optimal vision platform with its 8" large optics dome and excellent field of view.

WING AND TAIL PLANFORMS

The specifics of the wing design were optimized through the use of the Avatar Toolbox Spreadsheet in conjunction with XFLR5. The final parameters of the wing are shown below:

Inboard Wing	
Span	17 in
Area	258.4 in ²
Root Chord	16 in
Tip Chord	14.4 in
Aspect Ratio	1.12
Dihedral	10°
Incidence Angle	2°
Taper Ratio	.9
Sweep	2.5°
Airfoil	SD7034
Flaps	
Span	Full Inboard Span
Flap Chord Percentage	25%
Max Deflection	30°

Outboard Wing	
Span	43 in
Area	493.425 in ²
Root Chord	14.4 in
Tip Chord	10.08 in
Aspect Ratio	3.51
Dihedral	1.33°
Incidence Angle	2°
Wing Tip Twist	-1.5°
Sweep	5.4°
Taper Ratio	.7
Airfoil	SD7034
Ailerons	
Span	Full Outboard Span
Chord Percentage	20%
Max Deflection	±30°

Total Wing	
Span	120 in
Area	1569.44 in ²
Root Chord	16 in
Tip Chord	10.08 in
Aspect Ratio	9.18
Taper Ratio	0.63
MAC	13.3 in
MAC location span-wise	27.9 in
Dihedral	1.91°
Wing Loading	26.42 oz/ft ²
Cruise C _L	0.4

Inverted V Tail	
Project Vertical Span	11.9 in
Project Horizontal Span	34 in
Panel Span	20.75 in
Aspect Ratio	2.16
Area	398.46 in ²
MAC	9.8 in
Tail Angle	35°
Taper Ratio	0.6
Root Chord	12 in
Center Chord	7.2 in
Sweep	15°
Ruddervators	
Span	Full Tail Span
Chord Percentage	30%
Max Deflection	±30°

FUSELAGE DESIGN

The final design of the fuselage will consist of a two compartment structure each designed to carry different hardware components. The forward compartment will carry the camera system and the other necessary hardware to process and transfer the data acquired by the camera within a holding modulus. The back compartment will hold hardware imperative for autonomous and manual flight. The bottom of the fuselage will be reinforced to accommodate for the impact force generated when landing. This extra strength will be sufficient to support fixed landing gear of either bicycle or tricycle layout.



Figure 34: Aircraft Overhead View

AERODYNAMICS

The charts in the aerodynamics section of the report summarize the important aerodynamic values of the aircraft. Aerodynamic analysis has been done hand-in-hand with each element of the design process and is the essential driving factor of the entire design process. All aerodynamic factors are enumerated throughout the AVATAR Toolbox Spreadsheet.

MANUFACTURING CONSIDERATIONS

This section provides information regarding the considerations that were taken in the construction of the aircraft. The main components considered were the inboard wings and fuselage component, the outboard wings, and the tail. The preferred method of construction of the fuselage and tail is through a mold design. If budget permits the outboard wings will be constructed in a similar fashion however they will most likely be built in a foam core stencil process described in more detail in the manufacturing section. All of the components are to be constructed out of composite materials except the booms, which will be made out of carbon fiber tubes.

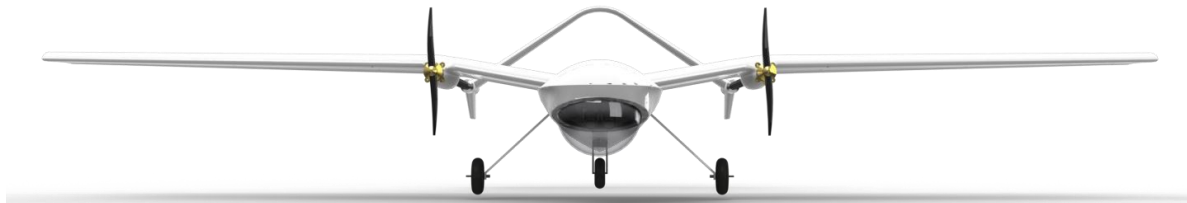


Figure 35: Aircraft Front View

COMPOSITE CONSTRUCTION

This section details the actual process that took place in the construction of the aircraft. As planned the tail and fuselage were produced through the use of molds. The molds themselves were also produced through a composite process. The outboard wings were constructed through the “remnant foam method.” Contrary to the manufacturing considerations and weight and sizing sections, the joints between the spars were carbon tube connectors and latches as opposed to the considered fork and pin method. The details of each process are further explored in the composite

construction section. An explanation of the current model of the aircraft is also provided in this section. A full display of the internal structure is shown in the figure below:

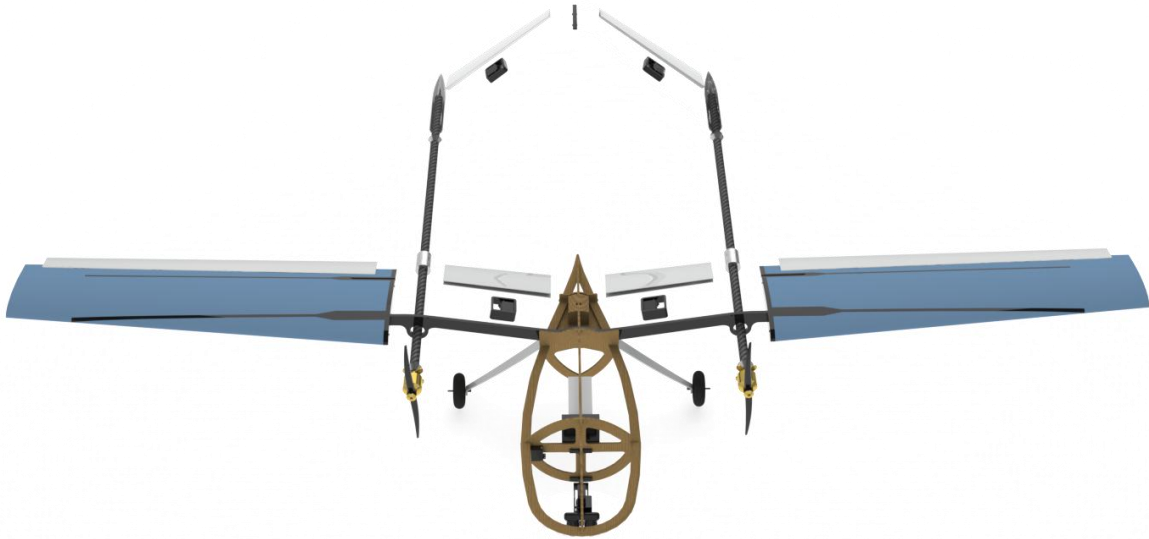


Figure 36: Full Internal Render

APPENDICES

APPENDIX A: 2011 AUVSI SUAS COMPETITION RULES

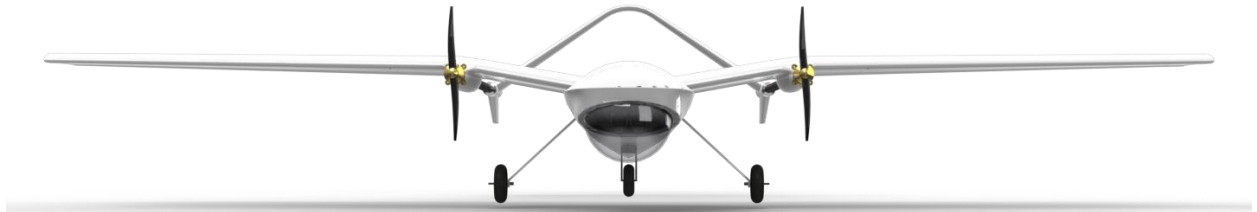
The competition rules can be found at this web address:

<http://pma263webdev.bowheadsupport.com/studentcomp2010/rules/2010RFP20090824_updated.pdf>

Item	Description	Part Number	Quantity	Unit Price	Total	URL
Servo Boosters	12" Boosted Extension	SC60005	2 cables	\$13.95	\$27.90	http://www.servotv.com/html/boosted_servo_extensions.html
Receiver batt	Receiver Pack 2700mah 6V NiMH Sanyo by JR	JRPB5008	2 batteries	\$43.99	\$87.98	http://www.horizonhobby.com/products/reviews.aspx?prodID=19995008&reviewsTab
Receiver switch	Wolverine Silver (2 Futaba in, 2 JR out)		1 unit	\$59.00	\$59.00	http://www.tromecor.com/products/04frcw-430/
Latche!!!!						http://www.sourtkco.com/products/07living-hinge-draw-latches/07-50-501-72.html
Pusher Prop	APC 14X8 SEP		2 props	\$7.33	\$14.66	http://www.apcprops.com/productDetails.asp?productcode=LP1408SEP
Traction Prop	APC 14X8 SE		2 props	\$4.89	\$9.78	http://www.apcprops.com/productDetails.asp?productcode=LP1408SE
P CARD 3						
Cheap Batts	ZIPPY Flightmax 5000mah 551P 15C	Z50005515C	6 battery	\$39.99	\$239.94	http://www.hobbyking.com/hobbyking/store/uh_viewItem.asp?idProduct=6499
P CARD 2	Motor/Prop/ESC:					
Motors	Hacker A50-12S Brushless Outrunner RC Motor, 395g, 1250W, 492 RPM/Volt		2 motors	\$109.99	\$219.98	http://www.amazon.com/Hacker-A50-12S-Brushless-Outrunner-Motor/dp/B00095YRQ2
ESCs	Hacker X-70 SB Pro Brushless Motor Speed Controller ESC 70A		2 escs	\$119.99	\$239.98	http://www.amazon.com/Hacker-Brushless-Motor-Speed-Controller/dp/B000UZYVWQ
				amt tot	459.96	
P CARD 1						
Servo Extenders	Hitec Alleron Extension 36"	LXVE95	4 cables	\$8.59	\$34.36	http://www.3towerhobbies.com/GfE-bin/w/10001978/LXVE95&P=Z
	Hitec Alleron Extension 24"	LXVE94	2 cables	\$8.59	\$17.18	http://www.3towerhobbies.com/GfE-bin/w/10001978/LXVE94&P=Z
Wheels	Dubro Treaded Lightweight Wheel 3" (2)	LXD780	1 set	\$9.69	\$9.69	http://www.3towerhobbies.com/GfE-bin/w/10001978/LXD780&P=FR
Servos	Hitec HS-5685MH High Volt High Torque Metal Gear Servo	HRCM5685	6 servos	\$54.99	\$329.94	http://www.3towerhobbies.com/GfE-bin/w/10001978/LXN7ZZ
	Hitec HS-311 Servo Standard U	LXD6LS	1 servo	\$7.99	\$7.99	http://www.3towerhobbies.com/GfE-bin/w/10001978/LXD6LS&P=VL
Main Landing Gear						
Wheels	Dubro Treaded Lightweight Wheel 4"	LXD783	2 sets	\$14.69	\$29.38	http://www.3towerhobbies.com/GfE-bin/w/10001978/LXD783&P=VL
Axles	Dubro Axle Shaft 3/16x2" (2)	LXD825	1 set	\$5.79	\$5.79	http://www.3towerhobbies.com/GfE-bin/w/10001978/LXD825&P=M
Collars	Dubro Dura-Collars 3/16" (4)	LXD835	1 set	\$1.89	\$1.89	http://www.3towerhobbies.com/GfE-bin/w/10001978/LXD835&P=M
Control Horns	Great Planes Control Horn Large Scale (2)	LXA6E	3 sets	\$3.19	\$9.57	http://www.3towerhobbies.com/GfE-bin/w/10001978/LXA6E&P=M
Connection Stuff						
	Dubro Full Threaded Rod 4-40 12" (12)	LXD872	1 set	\$18.19	\$18.19	http://www.3towerhobbies.com/GfE-bin/w/10001978/LXD872&P=M
	Great Planes Threaded Locking Clevis 4-40 (12)	LXEC8	1 set	\$9.99	\$9.99	http://www.3towerhobbies.com/GfE-bin/w/10001978/LXEC8&P=Z
Landing Gear	Dual Strut Nose Gear	LXH134	1 set	\$26.99	\$26.99	http://www.3towerhobbies.com/GfE-bin/w/10001978/LXH134&P=VL
				TOT	\$500.96	

APPENDIX C: SOLIDWORKS 3D RENDERS





REFERENCES

1. Raymer, Daniel P. *Aircraft Design: a Conceptual Approach*. Reston, VA: American Institute of Aeronautics and Astronautics, 2006. Print.
2. Anderson, John D. *Fundamentals of Aerodynamics*. Boston: McGraw-Hill Higher Education, 2007. Print.
3. McCormick, Barnes Warnock. *Aerodynamics, Aeronautics, and Flight Mechanics*. New York: Wiley, 1995. Print.
4. Lennon, Andy. *Basics of R/C Model Aircraft Design: Practical Techniques for Building Better Models*. Wilton, CT: Air Age, 1996. Print.
5. Simons, Martin. *Model Aircraft Aerodynamics*. Poole, Dorset [England: Special Interest Model, 2002. Print.
6. Adkins, C. N.: *Design of Optimum Propellers*, AIAA-83-0190. Also published in the *Journal of Propulsion and Power*, Vol. 10, No. 5, September-October 1994.
7. X-andre. "XFLR5." [Http://sourceforge.net/](http://sourceforge.net/). Web. 06 Dec. 2010.
<<http://xflr5.sourceforge.net/>>.